Results Math (2025) 80:27
Online First

https://doi.org/10.1007/s00025-024-02346-6

Results in Mathematics

Area Preserving Combescure Transformations

Olimjoni Pirahmad, Helmut Pottmann, and Mikhail Skopenkov

Abstract. Motivated by the design of flexible nets, we classify all nets of arbitrary size $m \times n$ that admit a continuous family of area-preserving Combescure transformations. There are just two different classes. The nets in the first class are special cases of cone nets that have been recently studied by Kilian, Müller, and Tervooren. The second class consists of Kœnigs nets having a Christoffel dual with the same areas of corresponding faces. We apply isotropic metric duality to get a new class of flexible nets in isotropic geometry. We also study the smooth analogs of the introduced classes.

Mathematics Subject Classification. 53A70, 53A05, 52C25, 53A35.

Keywords. Area preserving Combescure transformation, deformation, cone-net, flexible mesh, Christoffel dual.

1. Introduction

The motivation for our paper originates from the search for flexible quadrilateral meshes. Considering the faces as rigid bodies and the edges where two faces meet as hinges, such meshes allow for continuous flexion. In other words, they are mechanisms. Very recently, there has been growing interest in this area, with applications in rigid origami and transformable design [1–9]. In our paper, we suggest a new approach to the problem.

We restrict to quad meshes of regular combinatorics and call them (discrete) *nets* in the following. The flexibility is interesting to study, starting from nets with 3×3 faces. The flexible 3×3 Q-nets (meshes with planar faces)

Olimjoni Pirahmad, Helmut Pottmann and Mikhail Skopenkov have contributed equally to this work.

Published online: 05 January 2025

have been classified in a seminal paper by Izmestiev [10], which revealed a big variety of types. Well-known examples of flexible Q-nets of arbitrary size $m \times n$ are the Voss nets and T-nets, treated in detail by R. Sauer [11]. Very recently, Nawratil [12] presented another special class of flexible Q-nets which he calls P-nets. They may be seen as a generalization of rotational nets and can be easily designed but cannot provide a large variety of shapes. Further important recent progress is due to He and Guest [13], who have been able to patch other types of 3×3 nets together to larger flexible Q-nets. However, this is not yet a method for the design of flexible structures since the result is hardly predictable by the provided generation process.

In view of the difficulties that arise in Euclidean geometry, we simplify the problem and turn our interest to isotropic geometry, which may be seen as a *structure-preserving degeneration* of Euclidean one. The examples found in isotropic geometry can then be used as a good initialization to construct Euclidean ones via numerical optimization. This approach has been (implicitly) used since as early as the work [14] by Müntz from 1911, who solved the Plateau problem for Euclidean minimal surfaces in a quite general setup by deformation of isotropic minimal surfaces (graphs of harmonic functions). Another successful example of a structure-preserving degeneration is tropical geometry.

The geometry in *isotropic 3-space* I^3 is based on a 6-parametric group of affine transformations in $\mathbb{R}^3$ which preserve the isotropic semi-norm $\|(x, y, z)\|_i := \sqrt{x^2 + y^2}$. This geometry has been systematically developed by K. Strubecker [15–18]. A detailed treatment is found in the monograph by H. Sachs [19]. The geometry in I^3 is not as degenerate as it may appear by just looking at the metric. One can come up with so-called replacing invariants and obtain beautiful counterparts to Euclidean results. For example, one finds a definition of isotropic Gaussian curvature K_i of a surface that has properties very similar to the familiar Euclidean counterpart. However, pursuing the Riemannian approach based on the isotropic metric, K_i would vanish everywhere. Isotropic curvature theory of surfaces defines a counterpart to the Euclidean shape operator via an isotropic Gauss map that maps a surface via parallel tangent planes to the parabolic isotropic unit sphere $S_i^2 : 2z = x^2 + y^2$. If the surface is a function graph $z = f(x, y)$, then K_i is the determinant of the Hessian, i.e., $K_i = f_{xx} f_{yy} - f_{xy}^2$.

Since flexible nets may be seen as discrete versions of continuous isometric deformations of a surface, one needs a proper definition of isometric surfaces in I^3, which has been missing until very recently. Requiring the preservation of the lengths of surface curves *and* of isotropic Gaussian curvature during an isometric deformation, one obtains the desired non-degenerate analog to the Euclidean case [20]. Unlike Euclidean geometry, isotropic geometry possesses a metric duality realized via the polarity δ with respect to S_i^2. It has been shown [20] that δ transforms a pair of isometric surfaces in I^3 to a pair of surfaces

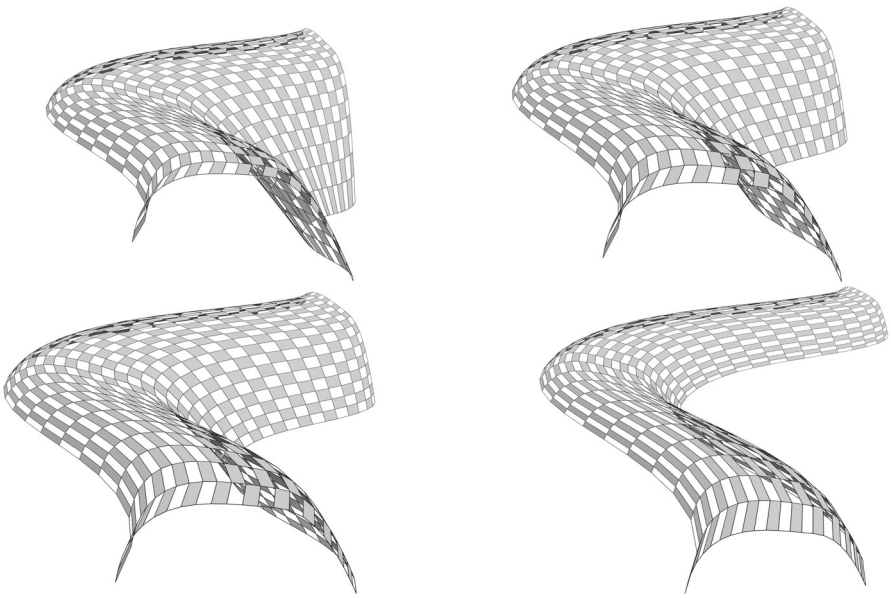

FIGURE 1. A sequence of deformations of a Q-net from class (i) in $\mathbb{R}^3$. Corresponding edges are parallel, and corresponding faces have equal areas. For a net from class (i), the two faces of each 1×2 sub-net or each 2×1 sub-net are affine symmetric. See Theorem 9

which are related by an *area-preserving Combescure transformation*. In the smooth setting, two surfaces $f(u, v)$ and $f^+(u, v)$ are related by a Combescure transformation (C-trafo), if corresponding tangent vectors f_u, f_u^+ and f_v, f_v^+ of parameter lines are parallel.

C-trafos play a fundamental role in discrete differential geometry [21]. Two Q-nets are related by a C-trafo if corresponding edges are parallel. Dual to the search for flexible Q-nets in I^3, we have to find all *Q-nets which allow for a continuous family of area preserving C-trafos*. In the following, we denote such Q-nets as *deformable*. See Fig. 1.

This problem is one of affine geometry in $\mathbb{R}^2$. Indeed, if two Q-nets are related by a C-trafo, corresponding faces are parallel, and we require that they have the same area. This implies immediately the following basic fact. If two Q-nets in $\mathbb{R}^d$, where $d \geq 3$, are related by an area-preserving C-trafo, the same is true for their images under any parallel projection into a plane. Conversely, any area preserving C-trafo in the plane can be lifted to $\mathbb{R}^d$ in infinitely many essentially different ways. We just add $d-2$ coordinates to the vertices of two transversal discrete parameter lines of one Q-net in the plane and complete the lifted nets via parallelism.

After having classified all deformable Q-nets in I^3, we will apply metric duality and obtain all flexible Q-nets in I^3. Then, our goal is to transform these nets with a numerical optimization algorithm to Euclidean flexible Q-nets. The latter is, however, the subject of a future publication.

1.1. Pointers to the Classical Literature

Area preserving maps between surfaces is a well-studied subject of classical differential geometry and cartography. In the latter case, the focus is on maps from the sphere to the plane.

Already the seemingly simple cases of area preserving maps on the sphere S^2 or in the Euclidean plane $\mathbb{R}^2$ possess a remarkable theory that reaches into non-Euclidean geometries. G. Fubini [22] found all area-preserving maps on S^2 via the so-called kinematic mapping of oriented lines L in elliptic 3-space E^3 to pairs (L_l, L_r) of points (left and right image) on S^2. For details on this map, which uses Clifford parallelism in E^3, we refer to [23,24]. The normal lines of a surface $\Phi \subset E^3$ get mapped to a left and right image domain Φ_l and Φ_r, respectively, which are related by an area preserving map. All smooth area-preserving maps on S^2 can be generated in this way.

Only after Fubini's result a similar construction of area preserving maps in the plane has been discovered. Based on initial work by G. Scheffers [25], K. Strubecker [18] developed the theory of the so-called *paratactic map* of contact elements C in isotropic 3-space I^3 to pairs of points (C_l, C_r) in the plane. A contact element is defined as a pair consisting of a point and an incident plane. The paratactic map is one application of the geometry in I^3. It possesses limits of Clifford translations which generate the paratactic map. Remarkably, if the contact elements are formed by the points plus tangent planes of a surface $\Phi \subset I^3$, the left and right images in the plane are related by an area preserving map. A special property related to our work is the following: Mapping the asymptotic net of a negatively curved surface Φ results in two nets related by a C-trafo. Hence, a negatively curved surface Φ generates an area preserving C-trafo $\Phi_l \mapsto \Phi_r$ between two nets in $\mathbb{R}^2$. Note that we are searching for a continuous family of nets related by area preserving C-trafos.

Another relevant result is Minkowski's theorem on the existence and uniqueness of a convex polytope with given directions and areas of faces. The polytope surface can be viewed as a mesh (with combinatorics more complex than a square grid), and then the theorem implies that the mesh admits no non-congruent area-preserving C-trafos. Via the metric duality δ, this translates to *isotropic Cauchy's theorem*: a mesh in I^3 whose metric dual is the surface of a convex polytope is not flexible.

1.2. Contributions and Overview

Our contributions in this paper are as follows.

In Sect. 2, we provide a classification of all deformable nets with 2×2 faces (3×3 vertices), since an $m \times n$ net is deformable if all 2×2 sub-nets are,

as we show later. This is in agreement with the fact that in I^3 (as in Euclidean $\mathbb{R}^3$) flexible Q-nets require flexible sub-nets of 3×3 faces, where only the 4 vertices of the inner face matter. Remarkably, *there are just two different classes*. See Theorem 1. The main part of the section presents the proof of the classification. It amounts to discussing a certain system of quadratic equations and identifying the cases where it has a one-parametric real solution. To keep our arguments elementary, we avoid tools such as complex projective space and resultants.

In Sect. 3, we classify deformable $m \times n$ nets and show how to build them from boundary data. See Theorem 9. All 2×2 sub-nets turn out to be of the same class. For class (i), the resulting nets are special cases of cone nets that have been recently studied by Kilian, Müller, and Tervooren [26]. Such nets also appeared in free-form architectural glass structures with planar quadrilateral (in fact trapezoidal) faces [27]. For class (ii), the resulting nets are special cases of well-known Kœnigs nets [21]. The class consists of nets having a Christoffel dual with the same areas of corresponding faces. While class (i) can yield visually pleasing discretizations of smooth deformable nets (see Fig. 1), class (ii) almost always exhibits the opposite behavior and a crumpled appearance (see Figs. 2 and 3).

This fact has a large impact when turning to smooth analogs in Sect. 4. The first class (i) yields smooth double cone nets where one family of cones are cylinders. The resulting surfaces are generalizations of translational surfaces, called scale-translational surfaces in architecture [27]. Ordinary translational surfaces appear as the only smooth analogs of the second class (ii). They constitute a special case of the smooth analogs of (i). Their metric duals in I^3 are the isotropic counterparts of Voss nets.

In Sect. 5, we conclude the paper with a few remarks on the dual flexible Q-nets whose detailed study and possibly conversion to Euclidean flexible Q-nets through optimization shall form the content of a separate publication. The nets of class (i) are instances of or closely related to multi-conjugate nets in the sense of Bobenko et al. [28]. They are also of interest in architectural applications, as discussed in [29,30]. Those of class (ii) appear crumpled, which is a frequent effect in Euclidean flexible Q-nets such as Miura origami and generalizations (see, e.g., [13]).

2. Deformable 2×2 Nets

In this section, we introduce basic notions and characterize all deformable 2×2 nets, i.e., nets that admit a family of non-congruent area-preserving Combescure transformations. We state the Classification Theorem 1 in Sect. 2.1, discuss the geometry of deformable nets in Sect. 2.2, and give the proof in Sect. 2.3.

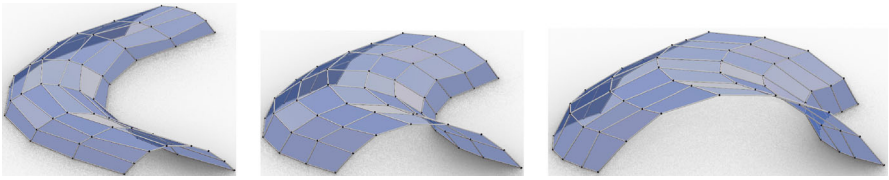

FIGURE 2. A sequence of deformations of a net from class (ii) in $\mathbb{R}^3$. Any two neighboring faces have equal so-called opposite ratios with respect to the common edge. See Sect. 2.1 and Theorem 9

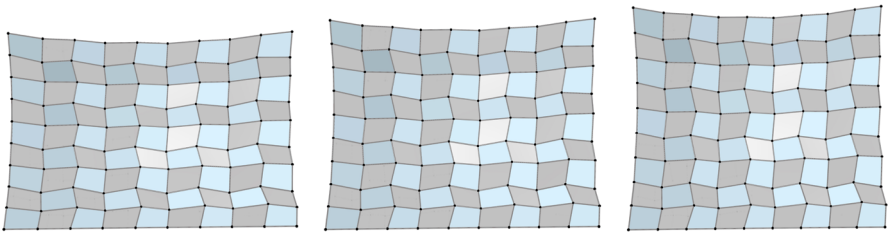

FIGURE 3. A sequence of deformations of a 9×9 net from class (ii) in $\mathbb{R}^3$. See Theorem 9

2.1. Statement of the Classification

Let us introduce basic notions. By an $m \times n$ *net* we mean a collection of $(m+1)(n+1)$ points $P_{ij} \in \mathbb{R}^d$ indexed by two integers $0 \le i \le m$ and $0 \le j \le n$ (i.e., a map $\{0, \dots, m\} \times \{0, \dots, n\} \to \mathbb{R}^d$), such that $P_{ij}, P_{i+1,j}, P_{i+1,j+1}, P_{i,j+1}$ are consecutive vertices of a convex quadrilateral for all $0 \le i < m$ and $0 \le j < n$. See Fig. 4. The latter quadrilaterals are called *faces*, and their sides are called *edges*. Faces and edges are *labeled*, i.e., equipped with an assignment of indices to their vertices (see [31, §2] for a detailed discussion of labeled polygons). An $m \times n$ net has mn faces, thus the name.

Edges or faces spanned by points with the same indices in two $m \times n$ nets are called *corresponding*. Two $m \times n$ nets are *parallel* or *Combescure transformations* of each other if their corresponding edges are parallel. Two $m \times n$ nets are *congruent*, if there is an isometry of $\mathbb{R}^d$ taking each point of the first net to the point of the second net with the same indices.

We come to the main notion of the paper.

Definition 1. (See Fig. 4) An $m \times n$ net is *deformable* if contained in a continuous family of pairwise non-congruent parallel $m \times n$ nets with the same areas of corresponding faces. Any member of this family is called a *deformation* of the initial net.

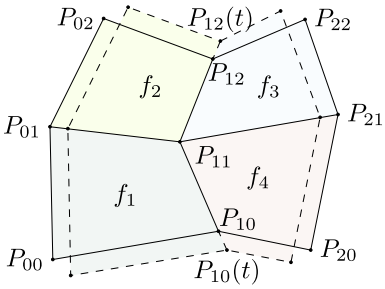

FIGURE 4. A 2×2 net (solid lines) and its deformation (dashed lines). Corresponding edges are parallel and corresponding faces (colored with the same color) have equal areas. See Definition 1

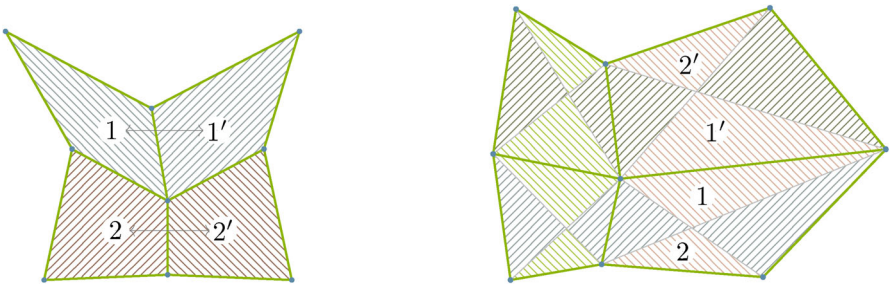

FIGURE 5. Two classes of deformable 2×2 nets introduced in Theorem 1. Left: class (i). Quadrilaterals in each pair $1, 1'$ and $2, 2'$ are affine symmetric, i.e., there exist two affine maps: one maps 1 to $1'$ and the other maps 2 to $2'$, keeping the points of the common sides fixed. Right: class (ii). Two pairs of red triangles $1, 2$ and $1', 2'$ have equal area ratios. This property holds for other pairs of triangles with the same color

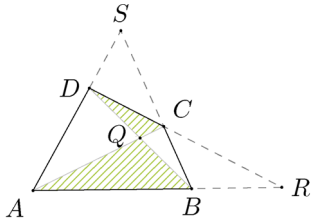

FIGURE 6. The opposite ratio of the quadrilateral $ABCD$ with respect to the side AB is the ratio of the areas of the colored triangles. See Proposition 8 for equivalent definitions

To state the classification theorem, we need a convention and two auxiliary notions.

The points of an $m \times n$ net need not be distinct. To deal with coincident points, we have labeled faces and edges. Faces or edges with different labels are viewed as distinct even if they coincide as subsets of $\mathbb{R}^d$. In particular, a common edge of two faces must have common labels with both.

A pair of quadrilaterals in $\mathbb{R}^d$ with a common side is called *affine symmetric with respect to the common side* if there is an affine map taking the first quadrilateral to the second one and keeping the points of the common side fixed. (Labels, if any, are ignored.) See Fig. 5(left) for an illustration.

The ratio of the areas of triangles AQB and CQD in a quadrilateral $ABCD$ with the diagonals meeting at Q is called the *opposite ratio of the quadrilateral $ABCD$ with respect to the side AB*. See Figs. 5(right) and 6. Notice that if two quadrilaterals are affine symmetric with respect to the common side, then their opposite ratios with respect to all corresponding sides are equal.

Theorem 1. *A 2×2 net is deformable if and only if at least one of the following conditions holds:*

(i) *the four faces split into two pairs that are affine symmetric with respect to the common edges;*
(ii) *each pair of faces with a common edge has equal opposite ratios with respect to that edge.*

The reader interested in the proof of the theorem can proceed directly to Sect. 2.3, and now we discuss geometric properties of resulting classes (i)–(ii) of deformable 2×2 nets.

2.2. Geometric Properties

There are equivalent descriptions of classes (i) and (ii), providing additional insight and simple ways to check conditions (i) and (ii) of Theorem 1 for a given net.

2.2.1. Class (i). Let us start with class (i) and show that it indeed consists of deformable nets.

Example 1. A 2×2 net whose faces split into two pairs that are affine symmetric with respect to the common edges is deformable.

Proof. See Fig. 4 and enumerate the faces as shown there. Assume that both pairs of faces f_1, f_2 and f_3, f_4 are affine symmetric with respect to the common sides.

Fix the common vertex P_{11} of all the faces. Move the point P_{10} of the net slightly along the line $P_{11}P_{10}$ to a new position $P_{10}(t)$. On the resulting segment $P_{11}P_{10}(t)$, construct a new quadrilateral $f_1(t)$ with the same area and the same side directions as f_1. Consider the affine symmetry taking f_1 to f_2,

and apply it to $f_1(t)$. We get a quadrilateral $f_2(t)$ with the same area and the same side directions as f_2 because an affine map preserves the parallelism of lines and the ratio of areas. Also, $f_1(t)$ and $f_2(t)$ share a common side because the points of the line $P_{11}P_{01}$ are fixed by the affine symmetry.

Analogously construct a quadrilateral $f_4(t)$ and its image $f_3(t)$ under the affine symmetry taking f_4 to f_3. Then both pairs $f_4, f_4(t)$ and $f_3, f_3(t)$ have parallel sides and equal areas, and $f_3(t)$ and $f_4(t)$ share a common side. It remains to note that $f_2(t)$ and $f_3(t)$ also share a common side: indeed, both affine symmetries take P_{10} to P_{12} and preserve the ratio $P_{11}P_{10} : P_{11}P_{10}(t)$, hence they take $P_{10}(t)$ to the same point $P_{12}(t)$. Thus $f_1(t), f_2(t), f_3(t), f_4(t)$ together constitute a deformation of our net. □

Let us introduce a geometric characterization of affine symmetric quadrilaterals.

Proposition 2 (See Fig. 7). *Two convex planar quadrilaterals $ABCD$ and $ABC'D'$ in $\mathbb{R}^d$, where C, D, C', D' are non-collinear, are affine symmetric with respect to their common side AB, if and only if $CC' \parallel DD'$ and the lines AB, CD, $C'D'$ are concurrent or parallel. Moreover, if the two quadrilaterals are not coplanar, then the latter condition and the assumption that C, D, C', D' are non-collinear can be dropped.*

Proof. The 'only if' part. Let $ABCD$ and $ABC'D'$ be affine symmetric. Then there is an affine map that maps C, D to C', D', respectively, and preserves the points of the line AB. The map takes the intersection point $AB \cap CD$, if it exists, to $AB \cap C'D'$, which means that $AB, CD, C'D'$ are parallel or concurrent. In particular, $C \neq C'$ and $D \neq D'$, otherwise C, D, C', D' are collinear because $ABCD$ is convex. Since the affine map preserves ratios of parallel segments, by the Thales theorem, we get $CC' \parallel DD'$.

The 'if' part. Consider the affine map that maps the triangle ACB to $AC'B$. This map takes the line CD to $C'D'$ because $AB, CD, C'D'$ are concurrent or parallel. Since $CC' \parallel DD'$ and C, D, C', D' are non-collinear, by the Thales theorem, it follows that D is taken to D', and we are done. □

As a consequence, we get the following geometric characterization of class (i).

Proposition 3 (See Fig. 8). *Consider a 2×2 net with points P_{ij}, where $0 \leq i, j \leq 2$, such that each of the quadruples $P_{00}, P_{10}, P_{02}, P_{12}$ and $P_{10}, P_{20}, P_{12}, P_{22}$ is not collinear. The pairs of faces*

$$(P_{00}P_{10}P_{11}P_{01}, P_{01}P_{11}P_{12}P_{02}) \qquad \text{and} \qquad (P_{10}P_{20}P_{21}P_{11}, P_{11}P_{21}P_{22}P_{12})$$

are affine symmetric with respect to their common edges if and only if $P_{00}P_{02} \parallel P_{10}P_{12} \parallel P_{20}P_{22}$ and the lines in each of the triples $P_{00}P_{10}, P_{01}P_{11}, P_{02}P_{12}$ and $P_{10}P_{20}, P_{11}P_{21}, P_{12}P_{22}$ are parallel or concurrent. Moreover, if no two faces are coplanar, then the latter two conditions can be dropped.

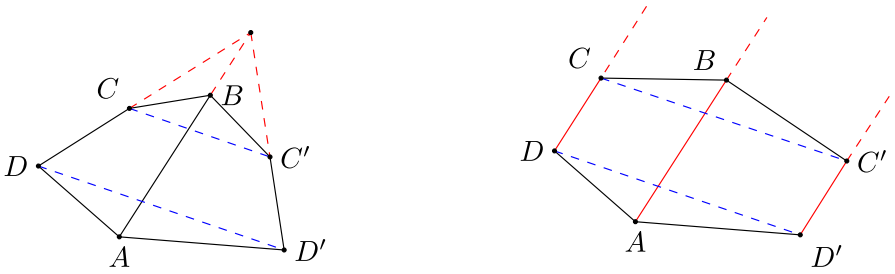

FIGURE 7. Properties of two affine symmetric quadrilaterals. Blue lines are parallel and red lines are either concurrent or parallel. See Proposition 2

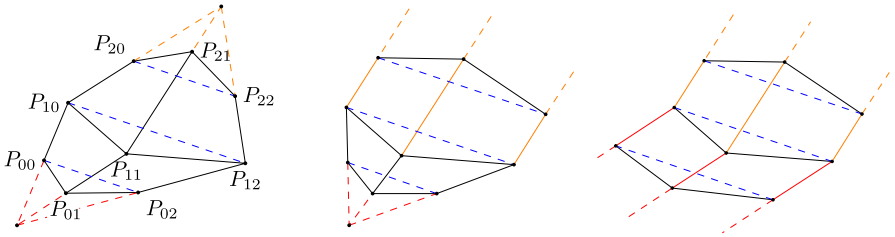

FIGURE 8. A geometric characterization of deformable 2×2 nets of class (i) in Theorem 1. Blue lines are parallel. Red and orange triples of lines are either concurrent or parallel. See Proposition 3

We shall see that each net of class (i) is a Kœnigs net. For Kœnigs nets, the condition that both triples $P_{00}P_{10}, P_{01}P_{11}, P_{02}P_{12}$ and $P_{10}P_{20}, P_{11}P_{21}, P_{12}P_{22}$ are parallel or concurrent implies that the triple $P_{00}P_{02}, P_{10}P_{12}, P_{20}P_{22}$ is parallel or concurrent (N. Affolter and A. Fairley, private communication). However, this does not yet imply that the net belongs to class (i) because the latter triple needs to be parallel.

2.2.2. Class (ii). The geometric description of class (ii) is less straightforward. To motivate it, we first briefly discuss a necessary condition for a 2×2 net to be deformable. This condition is actually the "infinitesimal deformability" studied in [20, §6.2]; cf. [32, §2.2] and [33, §2].

Let $P_{ij}(t)$ be a deformation of a 2×2 net P_{ij}, where $0 \le i, j \le 2$. Identify points in $\mathbb{R}^d$ with vectors. Assume that the derivatives $P'_{ij}(0)$ exist and do not all coincide. Consider the deformations $P_{ij}(t)P_{i+1,j}(t)P_{i+1,j+1}(t)P_{i,j+1}(t)$ of a particular face. These quadrilaterals have parallel sides and equal areas for all t. In particular, the derivative of the area at $t = 0$ vanishes. By a known computation [34, Theorem 13 and Eq. (3)], the latter is equivalent to quadrilaterals

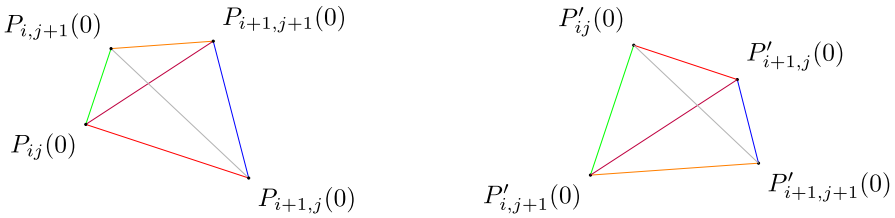

FIGURE 9. Dual quadrilaterals. Corresponding sides (with the same color) are parallel and non-corresponding diagonals (also with the same color) are parallel. See Sect. 2.2.2

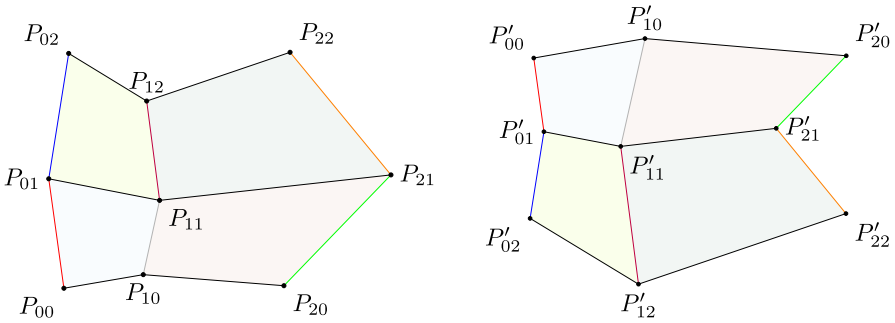

FIGURE 10. Two 2×2 nets that are Christoffel duals. Corresponding faces (of the same color) are dual

$P_{ij}(0)P_{i+1,j}(0)P_{i+1,j+1}(0)P_{i,j+1}(0)$ and $P'_{ij}(0)P'_{i+1,j}(0)P'_{i+1,j+1}(0)P'_{i,j+1}(0)$ being *dual*, i.e., having parallel corresponding sides and parallel non-corresponding diagonals (see Fig. 9):

$$P_{ij}(0)P_{i+1,j+1}(0) \parallel P'_{i+1,j}(0)P'_{i,j+1}(0),$$
$$P_{i+1,j}(0)P_{i,j+1}(0) \parallel P'_{ij}(0)P'_{i+1,j+1}(0).$$

This holds for all faces, hence points $P'_{ij}(0)$ form a 2×2 net, and the nets P_{ij} and $P'_{ij}(0)$ are *Christoffel duals*, i.e., their corresponding faces are dual. See Fig. 10. A net admitting a Christoffel dual is called a *Kœnigs* net. We conclude that an ("infinitesimally") deformable 2×2 net is a Kœnigs net.

Several geometric characterizations of Kœnigs nets are known. See Fig. 11. A 2×2 net with the vertices P_{ij}, where $0 \le i, j \le 2$, is a Kœnigs net, if and only if

$$\frac{P_{10}Q_{00}}{Q_{00}P_{01}} \cdot \frac{P_{01}Q_{01}}{Q_{01}P_{12}} \cdot \frac{P_{12}Q_{11}}{Q_{11}P_{21}} \cdot \frac{P_{21}Q_{10}}{Q_{10}P_{10}} = 1, \tag{1}$$

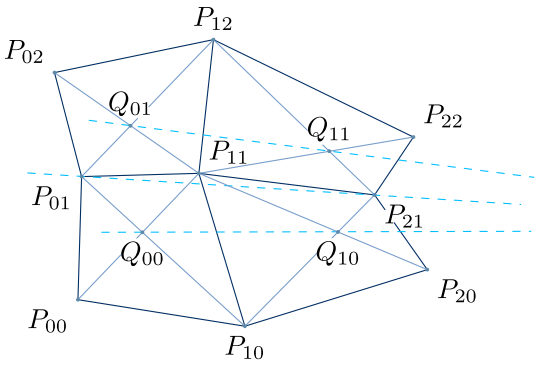

FIGURE 11. Three dashed lines for a deformable 2×2 net are either concurrent or parallel

where $Q_{ij} := P_{ij}P_{i+1,j+1} \cap P_{i+1,j}P_{i,j+1}$ for $0 \le i, j \le 1$ [21, Theorem 2.25]. If no three points among $P_{01}, P_{12}, P_{21}, P_{10}$ are collinear, then (1) is equivalent to the three lines $Q_{00}Q_{10}, P_{01}P_{21}, Q_{01}Q_{11}$ being concurrent or parallel [21, Theorem 9.12]. If the points $P_{01}, P_{12}, P_{21}, P_{10}$ are not coplanar, then the latter condition is equivalent to the coplanarity of $Q_{00}, Q_{01}, Q_{10}, Q_{11}$ [21, Theorem 2.26].

Proposition 4. *A 2×2 net satisfying one of conditions (i)–(ii) of Theorem 1 is a Kœnigs net.*

We give a direct elementary proof relying neither on infinitesimal deformability nor duality.

Proof. Enumerate the faces containing the points $Q_{00}, Q_{01}, Q_{11}, Q_{10}$ in the listed order so that the indices are cyclic modulo 4. Denote by $r(i, j)$ the opposite ratio of the i-th face with respect to its common edge with j-th face. Then $P_{10}Q_{00}/Q_{00}P_{01} = \sqrt{r(1,4)/r(1,2)}$ by a direct computation (see (5) below). Substituting similar expressions for the other factors in (1), we rewrite it in an equivalent form:

$$\frac{r(1,2)r(2,3)r(3,4)r(4,1)}{r(1,4)r(2,1)r(3,2)r(4,3)} = 1. \tag{2}$$

If the net is from class (i), then $r(i, j-1) = r(i-1, j)$ either for all even i, j or for all odd i, j, because affine symmetric quadrilaterals have equal opposite ratios with respect to corresponding edges.

If the net is from class (ii), then $r(i, j) = r(j, i)$ for all i, j different by 1.

In both cases, the numerator and the denominator of (2) cancel out completely, as required. □

To describe class (ii) geometrically, we return to the duality. Notice that a Christoffel dual of a 2×2 net is one of its Combescure transformations.

Now we show the following: if this particular Combescure transformation is area-preserving, then there is a whole family of area-preserving Combescure transformations, and this happens exactly for nets from class (ii).

Proposition 5. *If a* 2×2 *net* P_{ij} $(0 \le i, j \le 2)$ *has a Christoffel dual* P^*_{ij} $(0 \le i, j \le 2)$ *with the same areas of corresponding faces, then*

$$P_{ij}(t) = P_{ij} \cosh t + P^*_{ij} \sinh t, \qquad t \in [0, \varepsilon], 0 \le i, j \le 2, \tag{3}$$

is a family of area-preserving Combescure transformations for sufficiently small $\varepsilon > 0$.

Proof. Clearly, the nets P_{ij}, P^*_{ij}, and $P_{ij}(t)$ are parallel. Let f, f^*, and $f(t)$ be their corresponding faces. Dual quadrilaterals f and f^* have opposite orientation, hence opposite oriented areas $\mathrm{Area}(f^*) = -\mathrm{Area}(f)$. Their mixed area $\mathrm{Area}(f, f^*) = 0$ by [34, Theorem 13]. Then by [34, Eq. (3)], we get

$$\mathrm{Area}(f(t)) = \mathrm{Area}(f) \cosh^2 t + \mathrm{Area}(f^*) \sinh^2 t + 2\mathrm{Area}(f, f^*) \cosh t \sinh t = \\ = \mathrm{Area}(f) = \mathrm{const}.$$

□

In this construction, opposite ratios arise as follows.

Proposition 6. *If two dual convex quadrilaterals* f *and* f^* *have equal areas, then the ratio of their corresponding sides* e *and* e^* *equals the square root of the opposite ratio of* f *with respect to* e.

Proof. (Cf. [21, Proof of Lemma 2.20].) Let A, B, C, D be consecutive vertices of f so that $AB = e$, let Q be the intersection point of the diagonals, e_1 and e_2 be some vectors along the diagonals,

$$\overrightarrow{QA} = \alpha e_1, \quad \overrightarrow{QB} = \beta e_2, \\ \overrightarrow{QC} = \gamma e_1, \quad \overrightarrow{QD} = \delta e_2.$$

Since f is convex, we may assume that $\alpha\beta\gamma\delta = 1$ without loss of generality.

Construct a quadrilateral $A^*B^*C^*D^*$ with the intersection of the diagonals Q^* by setting

$$\overrightarrow{Q^*A^*} = -\frac{e_2}{\alpha}, \quad \overrightarrow{Q^*B^*} = -\frac{e_1}{\beta}, \\ \overrightarrow{Q^*C^*} = -\frac{e_2}{\gamma}, \quad \overrightarrow{Q^*D^*} = -\frac{e_1}{\delta} \qquad [21, \text{Eq. } (2.28)].$$

The resulting quadrilateral is dual to f and has the same area because $\alpha\beta\gamma\delta = 1$. Since the quadrilateral dual to a given one is unique up to scaling and translation [21, Lemma 2.20], we may assume that $f^* = A^*B^*C^*D^*$ so that $e^* = A^*B^*$.

By the similarity of ABQ and $A^*B^*Q^*$, the ratio of e and e^* equals $AB/A^*B^* = |\alpha\beta|$. The opposite ratio of f with respect to e is $|\alpha\beta|/|\gamma\delta| = |\alpha\beta|^2$, as required. □

As a consequence, we get the following characterization of class (ii). See Figs. 5(right) and 10.

Proposition 7. *For a 2×2 net, the following two conditions are equivalent:*

- *each pair of faces with a common edge has equal opposite ratios with respect to that edge;*
- *the net has a Christoffel dual with the same areas of corresponding faces.*

Proof. Each face has a dual quadrilateral of the same area [21, Lemma 2.20]. Performing a central symmetry, if necessary, we may assume that for any edge of the form $P_{ij}P_{i+1,j}$, the corresponding oriented side of the dual quadrilateral has the same direction, and for any edge of the form $P_{ij}P_{i,j+1}$, the corresponding oriented side has the opposite direction. See Fig. 9. The resulting dual quadrilaterals are unique up to translation. By Proposition 6, their oriented sides fit to compose a whole Christoffel dual net if and only if the required opposite ratios are equal. □

Propositions 5 and 7 show that class (ii) indeed consists of deformable nets.

2.2.3. Opposite Ratios. Let us discuss further properties of the opposite ratio. See Fig. 6. First, the opposite ratio is the product of the *diagonal-ratios* $[AQ/QC]$ and $[BQ/QD]$ studied in [35]:

Proposition 8. *If the rays BC and AD extending the sides of a convex quadrilateral $ABCD$ meet at a point S and the diagonals meet at Q, then the opposite ratio of $ABCD$ with respect to AB is*

$$\begin{aligned}\frac{\operatorname{Area}(AQB)}{\operatorname{Area}(CQD)} &= \frac{AQ \cdot BQ}{CQ \cdot DQ} = \frac{AS \cdot BS}{CS \cdot DS} \\ &= \frac{\operatorname{Area}(ASB)}{\operatorname{Area}(CSD)} = \left(1 - \frac{\operatorname{Area}(ABCD)}{\operatorname{Area}(ABS)}\right)^{-1}. \end{aligned} \tag{4}$$

Proof. The second equality follows from Menelaus' theorem for the triangles ADQ and BCQ:

$$\frac{AS}{DS} = \frac{BQ}{BD} \cdot \frac{CA}{CQ} \quad \text{and} \quad \frac{BS}{CS} = \frac{AQ}{AC} \cdot \frac{DB}{DQ}.$$

The other three equalities are straightforward. □

Thus, in particular, rays BC and AD intersect if and only if this opposite ratio is greater than 1.

Further, just like (4) expresses the opposite ratio in terms of certain length ratios, those length ratios themselves can be expressed in terms of opposite ratios:

$$\frac{AQ}{CQ} = \sqrt{\frac{\operatorname{Area}(AQB)}{\operatorname{Area}(CQD)} \cdot \frac{\operatorname{Area}(DQA)}{\operatorname{Area}(BQC)}}$$

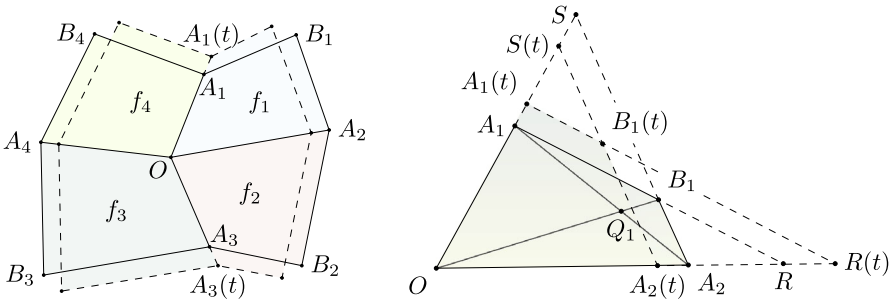

FIGURE 12. Notation used throughout Sect. 2.3 (left) and the proofs of Lemmas 1–2 (right)

$$\text{and} \quad \frac{BQ}{DQ} = \sqrt{\frac{\text{Area}(AQB)}{\text{Area}(CQD)} \cdot \frac{\text{Area}(BQC)}{\text{Area}(DQA)}}. \tag{5}$$

This shows that two opposite ratios of a quadrilateral with respect to two adjacent sides determine the quadrilateral uniquely up to affine transformations: given vertices A, B, C, the first equation uniquely determines Q, and the second one uniquely determines D. We arrive at the following corollary.

Corollary 1. *There exists a unique convex quadrilateral $ABCD$ with given (non-collinear) vertices A, B, C and given (positive) opposite ratios with respect to the sides AB and BC.*

This suggests the following construction of deformable 2×2 nets. A pair of opposite faces $P_{00}P_{01}P_{11}P_{10}$ and $P_{11}P_{12}P_{22}P_{21}$ can be prescribed arbitrarily as long as the triples P_{01}, P_{11}, P_{12} and P_{10}, P_{11}, P_{21} are non-collinear. Then the remaining pair of faces is uniquely determined by condition (ii) of Theorem 1, leading to a unique 2×2 net from class (ii). Analogously, the pair of opposite faces leads to at most two 2×2 nets from class (i), depending on which pairs of faces are affine symmetric.

2.3. Proof of the Classification

First, we reduce the classification of deformable 2×2 nets to solving a system of quadratic equations. We need the following notation. See Fig. 12 (left).

The faces of a 2×2 net are denoted by f_1, f_2, f_3, f_4 so that f_i and f_{i-1} have a common edge for $i = 1, 2, 3, 4$, and the indices are cyclic modulo 4. The common vertex of all the faces is denoted by O, and the common edge of f_i and f_{i-1} is denoted by OA_i. The vertex of f_i other than O, A_i, A_{i+1} is denoted by B_i.

The *simple ratio of a quadrilateral $ABCD$ with respect to the oriented side AB* is

$$\begin{cases} AB/RA, & \text{if the rays } BA \text{ and } CD \text{ intersect at a point } R; \\ 0, & \text{if } AB \parallel CD; \\ -AB/RA, & \text{if the rays } AB \text{ and } DC \text{ intersect at a point } R \text{(see Fig. 6)}. \end{cases}$$

The simple ratios of the face f_i with respect to OA_i and OA_{i+1} are denoted by l_i and m_i respectively.

For two collinear vectors $\overrightarrow{AB}$ and $\overrightarrow{CD}$, denote by $\overrightarrow{AB}/\overrightarrow{CD}$ the number k such that $\overrightarrow{AB} = k \cdot \overrightarrow{CD}$.

Lemma 1. *A 2×2 net is deformable if and only if the system of equations*

$$P_i(x_i, x_{i+1}) := l_i x_i^2 + 2x_i x_{i+1} + m_i x_{i+1}^2 - (l_i + m_i + 2) = 0 \tag{6}$$

for $i = 1, 2, 3, 4$ has a non-constant continuous family of real solutions $\big(x_1(t), \dots, x_4(t)\big)$ with $x_1(0) = \cdots = x_4(0) = 1$.

Remark 1. Each such family determines a family of parallel nets with $OA_i(t)/OA_i = x_i(t)$.

Proof. Let us prove the following expression for the ratio of oriented areas:

$$\frac{\mathrm{Area}(OA_1B_1A_2)}{\mathrm{Area}(OA_1A_2)} = \frac{l_1 + m_1 + 2}{1 - l_1 m_1}. \tag{7}$$

Indeed, first assume that the lines OA_1, OA_2 intersect with A_2B_1, A_1B_1 at some points S, R, respectively. See Fig. 12(right). Then $\overrightarrow{OA_2}/\overrightarrow{OR} = -m_1$ and $\overrightarrow{OA_1}/\overrightarrow{OS} = -l_1$. By the Menelaus theorem for points A_2, B_1, S on the extensions of the sides of the triangle OA_1R, we get

$$\frac{\overrightarrow{A_1R}}{\overrightarrow{B_1R}} = 1 + \frac{\overrightarrow{A_1B_1}}{\overrightarrow{B_1R}} = 1 + \frac{\overrightarrow{SA_1}}{\overrightarrow{OS}} \cdot \frac{\overrightarrow{OA_2}}{\overrightarrow{RA_2}} = 1 - (1 + l_1) \cdot \frac{m_1}{1 + m_1} = \frac{1 - l_1 m_1}{1 + m_1}.$$

Then

$$\frac{\mathrm{Area}(OA_1B_1A_2)}{\mathrm{Area}(OA_1A_2)} = \frac{\mathrm{Area}(OA_1R)}{\mathrm{Area}(OA_1A_2)} - \frac{\mathrm{Area}(A_2B_1R)}{\mathrm{Area}(OA_1A_2)} = \frac{\overrightarrow{OR}}{\overrightarrow{OA_2}} - \frac{\overrightarrow{A_2R}}{\overrightarrow{OA_2}} \cdot \frac{\overrightarrow{B_1R}}{\overrightarrow{A_1R}} =$$

$$= -\frac{1}{m_1} - \frac{1 + m_1}{-m_1} \cdot \frac{1 + m_1}{1 - l_1 m_1} = \frac{l_1 + m_1 + 2}{1 - l_1 m_1}.$$

This proves (7) unless $OA_1B_1A_2$ has a pair of parallel sides. In the latter case, (7) is established, e.g., by a limiting argument.

Now assume that the net is deformable. Without loss of generality, assume that O is fixed during the deformation. In a deformation, take the face $OA_1(t)B_1(t)A_2(t)$ with the same area and the same side directions as $OA_1B_1A_2$. Denote $x_1(t) = OA_1(t)/OA_1$ and $x_2(t) = OA_2(t)/OA_2$. Then the simple ratios of the face $OA_1(t)B_1(t)A_2(t)$ with respect to the sides $OA_1(t)$

and $OA_2(t)$ are $l_1(t) = l_1 x_1(t)/x_2(t)$ and $m_1(t) = m_1 x_2(t)/x_1(t)$ respectively. Applying (7) two times, we get

$$\begin{aligned}\frac{l_1 + m_1 + 2}{1 - l_1 m_1} &= \frac{\mathrm{Area}(OA_1B_1A_2)}{\mathrm{Area}(OA_1A_2)} \\ &= \frac{\mathrm{Area}(OA_1(t)B_1(t)A_2(t))}{\mathrm{Area}(OA_1(t)A_2(t))} \cdot \frac{\mathrm{Area}(OA_1(t)A_2(t))}{\mathrm{Area}(OA_1A_2)} = \\ &= \frac{l_1(t) + m_1(t) + 2}{1 - l_1(t)m_1(t)} x_1(t)x_2(t) = \frac{l_1 x_1(t)^2 + 2x_1(t)x_2(t) + m_1 x_2(t)^2}{1 - l_1 m_1}.\end{aligned}$$

We have arrived at $P_1(x_1(t), x_2(t)) = 0$. Analogously we get (6) for $i = 2, 3, 4$.

Conversely, given a family of solutions of (6), we construct a family of parallel nets with the same areas of faces: the point O is fixed; the points $A_i(t)$ are determined by $OA_i(t)/OA_i = x_i(t)$. □

Conditions (i)–(ii) in Theorem 1 are restated in terms of the simple ratios l_i and m_i as follows.

Lemma 2. *For $i = 1, 2, 3, 4$, we have $l_i + 1, m_i + 1, 1 - l_i m_i > 0$. Two faces f_i and f_{i+1}:*

(i) *are affine symmetric with respect to their common edge if and only if $l_i = m_{i+1}$ and $l_{i+1} = m_i$;*
(ii) *have equal opposite-ratios with respect to their common edge if and only if*

$$\frac{1 - m_i l_i}{(1 + l_i)^2} = \frac{1 - m_{i+1} l_{i+1}}{(1 + m_{i+1})^2}.$$

The latter two fractions are the expressions for the opposite ratios in terms of the simple ratios.

Proof. Assume without loss of generality that $i = 1$.

First, we derive a useful expression for $l_1 + 1, m_1 + 1$, and $1 - l_1 m_1$. Let Q_1 be the intersection point of the diagonals of $OA_1B_1A_2$ and let $S = OA_1 \cap A_2B_1$ (if the latter lines are not parallel). See Fig. 12(right). Using Menelaus' theorem for points A_2, B_1, S and the triangle A_1Q_1O, we get

$$l_1 + 1 = \frac{\overrightarrow{A_1O}}{\overrightarrow{OS}} + 1 = \frac{\overrightarrow{A_1S}}{\overrightarrow{OS}} = \frac{\overrightarrow{A_1A_2}}{\overrightarrow{Q_1A_2}} \cdot \frac{\overrightarrow{B_1Q_1}}{\overrightarrow{B_1O}}.$$

Notice that the resulting expression remains true, even if $OA_1 \parallel A_2B_1$. Similarly, we have

$$m_1 + 1 = \frac{\overrightarrow{A_2A_1}}{\overrightarrow{Q_1A_1}} \cdot \frac{\overrightarrow{B_1Q_1}}{\overrightarrow{B_1O}}.$$

Substituting l_1+1, m_1+1 into $1-l_1m_1 = (m_1+1)[1-(l_1+1)+(l_1+1)/(m_1+1)]$, we get

$$1 - l_1m_1 = \frac{\overrightarrow{A_2A_1}}{\overrightarrow{Q_1A_1}} \cdot \frac{\overrightarrow{B_1Q_1}}{\overrightarrow{B_1O}} \cdot \left(1 - \frac{\overrightarrow{A_1A_2}}{\overrightarrow{Q_1A_2}} \cdot \frac{\overrightarrow{B_1Q_1}}{\overrightarrow{B_1O}} - \frac{\overrightarrow{Q_1A_1}}{\overrightarrow{Q_1A_2}}\right)$$
$$= \frac{\overrightarrow{A_2A_1}}{\overrightarrow{Q_1A_1}} \cdot \frac{\overrightarrow{B_1Q_1}}{\overrightarrow{B_1O}} \cdot \frac{\overrightarrow{Q_1O}}{\overrightarrow{B_1O}} \cdot \frac{\overrightarrow{A_1A_2}}{\overrightarrow{Q_1A_2}}.$$

In particular, $m_1+1, l_1+1, 1-l_1m_1 > 0$ by the convexity.

We have analogous expressions for m_2+1, l_2+1, $1-l_2m_2$ in terms of the point $Q_2 = OB_2 \cap A_2A_3$.

(i) From those expressions, we get

$$\frac{m_1+1}{l_1+1} = \frac{\overrightarrow{A_2Q_1}}{\overrightarrow{Q_1A_1}}, \frac{l_2+1}{m_2+1} = \frac{\overrightarrow{A_2Q_2}}{\overrightarrow{Q_2A_3}},$$
$$\frac{1}{m_1+1} + \frac{1}{l_1+1} = \frac{\overrightarrow{B_1O}}{\overrightarrow{B_1Q_1}}, \frac{1}{m_2+1} + \frac{1}{l_2+1} = \frac{\overrightarrow{B_2O}}{\overrightarrow{B_2Q_2}}.$$

Then $(l_1, m_1) = (m_2, l_2)$ is equivalent to

$$\frac{\overrightarrow{A_2Q_1}}{\overrightarrow{Q_1A_1}} = \frac{\overrightarrow{A_2Q_2}}{\overrightarrow{Q_2A_3}} \quad \text{and} \quad \frac{\overrightarrow{B_1O}}{\overrightarrow{B_1Q_1}} = \frac{\overrightarrow{B_2O}}{\overrightarrow{B_2Q_2}}. \tag{8}$$

Consider the affine map taking the triangle OB_1A_2 to OB_2A_2. Condition (8) means that the affine map takes A_1 to A_3. The latter is equivalent to $OA_1B_1A_2$ and $OA_2B_2A_3$ being affine symmetric.

(ii) Substituting expressions for $l_1+1, m_2+1, 1-l_1m_1, 1-l_2m_2$, we get

$$\frac{1-m_1l_1}{(1+l_1)^2} = \frac{\overrightarrow{Q_1A_2}}{\overrightarrow{Q_1A_1}} \cdot \frac{\overrightarrow{Q_1O}}{\overrightarrow{Q_1B_1}} \quad \text{and} \quad \frac{1-m_2l_2}{(1+m_2)^2} = \frac{\overrightarrow{Q_2A_2}}{\overrightarrow{Q_2A_3}} \cdot \frac{\overrightarrow{Q_2O}}{\overrightarrow{Q_2B_2}}.$$

The right sides are equal to the opposite ratios of the quadrilaterals $OA_1B_1A_2$ and $OA_2B_2A_3$ with respect to their common side OA_2. □

This restatement of conditions (i)–(ii) of Theorem 1 gives another proof that they are sufficient.

Example 2. A 2×2 net satisfying one of conditions (i)–(ii) in Theorem 1 is deformable. Moreover, for any edge, there is a deformation increasing its length and a deformation decreasing it.

Proof. By Lemma 1, it suffices to construct a family of solutions of system (6).

(i) Let both pairs f_1, f_2 and f_3, f_4 be affine symmetric with respect to the common sides. Then by Lemma 2(i) we get $l_1 = m_2$, $l_2 = m_1$, $l_3 = m_4$, $l_4 = m_3$. For $m_1, m_3 \neq 0$, we get the following family:

$$x_1(t) = 1+t, \quad x_2(t) = \frac{-(1+t) + \sqrt{(1+t)^2(1-l_1m_1) + m_1(l_1+m_1+2)}}{m_1},$$

$$x_3(t) = 1 + t, \quad x_4(t) = \frac{-(1+t) + \sqrt{(1+t)^2(1 - l_3 m_3) + m_3(l_3 + m_3 + 2)}}{m_3}.$$

The expressions under the roots are positive for small enough $|t|$ because for $t = 0$ they equal $(m_1 + 1)^2$ and $(m_3 + 1)^2$, hence are positive by Lemma 2. For $m_1 = 0$ or $m_3 = 0$, we set $x_2(t) = (1 - l_1 t - l_1 t^2/2)/(1 + t)$ or $x_4(t) = (1 - l_3 t - l_3 t^2/2)/(1 + t)$ respectively.

(ii) Let the equal opposite ratios of f_i and f_{i+1} be $1/k_{i+1}^2$, where $k_{i+1} > 0$, for $i = 1, 2, 3, 4$ with $k_5 = k_1$. Then by Lemma 2(ii) we get (see an automated checking in [36, Section 1])

$$l_i = \frac{k_{i+1}^2 - 1}{1 + k_i k_{i+1}} \quad \text{and} \quad m_i = \frac{k_i^2 - 1}{1 + k_i k_{i+1}}.$$

We get the following family of solutions of system (6) (see [36, Section 2]):

$$x_1(t) = \frac{(1+t)^2(1 - k_1) + 1 + k_1}{2(1+t)}, \quad x_2(t) = \frac{(1+t)^2(1 + k_2) + 1 - k_2}{2(1+t)},$$
$$x_3(t) = \frac{(1+t)^2(1 - k_3) + 1 + k_3}{2(1+t)}, \quad x_4(t) = \frac{(1+t)^2(1 + k_4) + 1 - k_4}{2(1+t)}.$$

The 'moreover' part holds for the edge OA_1 because $x_1'(0) \neq 0$ in both cases (i) and (ii). It remains to notice that if an area-preserving Combescure transformation increases the length of an edge, then it decreases the length of any adjacent edge in the same face. □

To show that conditions (i)–(ii) in Theorem 1 are necessary, consider space $\mathbb{R}^3$ with the coordinates x_1, x_2, x_3. Equations (6) for $i = 1$ and 2 define two cylinders, each being centrally symmetric with respect to the origin O. Denote by C_1 their intersection. Analogously define the sets C_i in space with the coordinates x_i, x_{i+1}, x_{i+2} for $i = 2, 3, 4$, where the indices are cyclic modulo 4. Those sets are (affine) algebraic curves of degree at most 4, which can have several components. We first consider the case when each curve $C_1, \dots, C_4$ contains a *conic*, i.e., an irreducible curve of degree 2.

Lemma 3. *The curve C_i contains a conic if and only if f_i and f_{i+1} have equal opposite ratios with respect to their common edge.*

Remark 2. In particular, by Lemma 2(ii), if $m_2 = l_1 = 0$ then C_1 contains a conic.

Proof. Assume without loss of generality that $i = 1$.

Let us prove the 'only if' part. Consider a conic contained in C_1. It is a plane section of the cylinder $P_1(x_1, x_2) = 0$, which is hyperbolic because the discriminant $1 - m_1 l_1 > 0$ by Lemma 2. Hence the conic is a hyperbola. Its center is the intersection of the axes $x_1 = x_2 = 0$ and $x_2 = x_3 = 0$ of the two cylinders $P_1(x_1, x_2) = 0$ and $P_2(x_2, x_3) = 0$ with the plane of the conic. Hence the center is the origin O. Consider the quadric

$$(l_2 + m_2 + 2)P_1(x_1, x_2) - (l_1 + m_1 + 2)P_2(x_2, x_3) = 0. \tag{9}$$

It contains the origin O and our conic. Hence it splits into one or two planes, both passing through the origin by central symmetry. Thus the determinant of the quadratic form in the left side of (9) is (see [36, Section 3])

$$(l_1+m_1+2)(l_2+m_2+2)\left((m_2+1)^2(1-m_1l_1)-(l_1+1)^2(1-l_2m_2)\right)=0. \tag{10}$$

The first two factors are nonzero by Lemma 2. By Lemma 2(ii), the desired opposite ratios are equal.

Let us prove the 'if' part. Assume that the opposite ratios are equal. Then by Lemma 2(ii) we get (10). If $l_1=m_2=0$, then C_1 contains the conic $(x_1(t),x_2(t),x_3(t))=\left(\frac{m_1+2-m_1t^2}{2t},t,\frac{l_2+2-l_2t^2}{2t}\right)$. Otherwise assume that $l_1\neq 0$ (the case $l_1=0$, $m_2\neq 0$ is similar). Then C_1 is contained in the quadric

$$(1-l_2m_2)l_1P_1(x_1,x_2)-(1-l_1m_1)m_2P_2(x_2,x_3)=(1-l_2m_2)(l_1x_1+x_2)^2-$$
$$-(1-l_1m_1)(x_2+m_2x_3)^2-(l_1+1)^2(1-l_2m_2)+(m_2+1)^2(1-l_1m_1)=0.$$

Here the free term vanishes by (10), and $1-l_1m_1, 1-l_2m_2>0$ by Lemma 2. Thus we get a product of two linear polynomials in x_1,x_2,x_3, and the quadric is the union of two planes. Then C_1 is the intersection of the planes with the cylinder $P_2(x_2,x_3)=0$, i.e., contains a conic. □

We have the following direct corollary.

Corollary 2. *If $C_1,\dots,C_4$ all contain conics, then condition (ii) of Theorem 1 holds.*

Now we turn to the case when one of the curves C_i, say, C_1, does not contain a conic. In this case we find the orthogonal projection of C_1 to the x_1x_3-plane, or, thinking algebraically, we eliminate x_2 from the system $P_1(x_1,x_2)=P_2(x_2,x_3)=0$. We need the following standard observation.

Lemma 4. *The orthogonal projection of an algebraic curve $C\subset\mathbb{R}^3$ to the x_1x_3-plane preserves the degree of C, if the projection is an injective map outside a finite subset, the inverse map is given by rational functions, and the projectivization of C does not contain the improper point of the projectivization of the x_2-axis.*

Proof. This is a step where we need slightly more advanced tools. We extend the projection to the complex projective space. Since the inverse map is given by rational functions, it also extends, and thus the projection remains injective. Take a plane passing through the improper point of the x_2-axis but not tangent to C and not containing the excluded and singular points of C. The plane has the same number of intersection points with C and its projection. By the Bezout theorem, we are done. □

We say that an algebraic equation is *reduced* if it has a minimal degree among all the equations with the same solution set in $\mathbb{R}^2$.

Lemma 5. *If C_1 does not contain a conic, then its orthogonal projection to the x_1x_3-plane is an irreducible curve (possibly with finitely many points excluded), given by one of the following equations:*

(a) *for $m_1 \neq 0$ or $l_2 \neq 0$, it is given by the reduced degree 4 equation*

$$\begin{vmatrix} m_1 & 0 & l_2 & 0 \\ 2x_1 & m_1 & 2x_3 & l_2 \\ l_1x_1^2 - l_1 - m_1 - 2 & 2x_1 & m_2x_3^2 - l_2 - m_2 - 2 & 2x_3 \\ 0 & l_1x_1^2 - l_1 - m_1 - 2 & 0 & m_2x_3^2 - l_2 - m_2 - 2 \end{vmatrix} = 0 \tag{11}$$

(b) *for $m_1 = l_2 = 0$, it is given by the reduced degree 3 equation*

$$l_1x_1^2x_3 - m_2x_3^2x_1 - (l_1 + 2)x_3 + (m_2 + 2)x_1 = 0. \tag{12}$$

Remark 3. In either case, the left side of (11)–(12) is the resultant of $P_1(x_1, x_2)$ and $P_2(x_2, x_3)$.

Proof. Notice that C_1 contains no straight lines; otherwise, this line lies in both cylinders and hence is parallel to both axes Ox_1 and Ox_3, which is impossible.

(a): Assume that $m_1 \neq 0$ without loss of generality. Eliminate the terms quadratic in x_2 from the system $P_1(x_1, x_2) = P_2(x_2, x_3) = 0$ by taking

$$\begin{aligned} l_2P_1(x_1, x_2) - m_1P_2(x_2, x_3) &= 2x_2(l_2x_1 - m_1x_3) + \\ &+ \underbrace{l_1l_2x_1^2 - m_1m_2x_3^2 + m_1m_2 - l_1l_2 + 2(m_1 - l_2)}_{Q(x_1,x_3)} = 0. \end{aligned} \tag{13}$$

Expressing x_2 (or better $2x_2(l_2x_1 - m_1x_3)$) through the resulting expression $Q(x_1, x_3)$ and substituting into the equation $4(l_2x_1 - m_1x_3)^2 \cdot P_1(x_1, x_2) = 0$, we get

$$\begin{aligned} &4(l_1x_1^2 - l_1 - m_1 - 2)(l_2x_1 - m_1x_3)^2 - 4x_1(l_2x_1 - m_1x_3)Q(x_1, x_3) + \\ &+m_1Q(x_1, x_3)^2 = 0. \end{aligned} \tag{14}$$

The resulting equation is equivalent to (11) (see [36, Section 4]) and describes a set *containing* the projection of C_1.

Let us show that the set actually *coincides* with the projection after removing finitely many points. Indeed, take an arbitrary (x_1, x_3) satisfying (14). Consider the following two possibilities.

If $l_2x_1 - m_1x_3 \neq 0$, then set $x_2 = -Q(x_1, x_3)/2(l_2x_1 - m_1x_3)$ so that (13) is satisfied. Then (14) implies $P_1(x_1, x_2) = 0$. Then by (13) we get $P_2(x_2, x_3) = 0$ because $m_1 \neq 0$. Thus $(x_1, x_2, x_3) \in C_1$ and (x_1, x_3) belongs to the projection of C_1.

If $l_2x_1 - m_1x_3 = 0$, then (14) implies $Q(x_1, x_3) = 0$. There are only finitely many such points (x_1, x_3) unless the linear polynomial $l_2x_1 - m_1x_3$ divides $Q(x_1, x_3)$. Let us show that the latter is impossible. Indeed, otherwise $l_2x_1 - m_1x_3$ divides the right side of (13) as well. Hence the latter splits into two linear factors, and (13) defines the union of two planes (possibly

coincident). Then C_1 is the intersection of those two planes with the cylinder $P_1(x_1, x_2) = 0$. Hence C_1 contains a conic or a line. This contradiction shows that curve (14) and the line $l_2x_1 - m_1x_3 = 0$ have finitely many common points, which we just drop.

Now we show that (14) is an irreducible curve of degree 4. Since C_1 does not contain conics or lines and has a degree at most 4, it follows that C_1 is irreducible of degree 4 or 3. Then curve (14) is also irreducible as a projection of an irreducible curve. However, equation (14) can a priori be non-reduced: its left side can be a complete square or cube or have a non-constant factor without real roots. In either case, curve (14) would have a degree at most 2. This would contradict to Lemma 4. The assumptions of the lemma hold because for $l_2x_1 - m_1x_3 \neq 0$, the second coordinate of a point $(x_1, x_2, x_3) \in C_1$ is uniquely determined by x_1 and x_3 via (13), the line $l_2x_1 - m_1x_3 = 0$ intersects curve (14) only at finitely many points by the above, and the projectivization of the cylinder $P_1(x_1, x_2) = 0$ does not contain the improper point of the x_2-axis by the assumption $m_1 \neq 0$. Thus (14) is reduced of degree 4 or 3. Computing the coefficients at x_3^4 and $x_1^2x_3^2$ and using $m_1 \neq 0$, we see that (14) has degree 4 unless $m_2 = l_1 = 0$. The latter possibility is ruled out by Remark 2.

(b): $m_1 = l_2 = 0$. In this case, we eliminate x_2 by taking

$$\begin{aligned} &x_3P_1(x_1, x_2) - x_1P_2(x_2, x_3) \\ &= l_1x_1^2x_3 - m_2x_3^2x_1 - (l_1 + 2)x_3 + (m_2 + 2)x_1 = 0. \end{aligned} \tag{15}$$

The resulting equation describes a set *containing* the projection of C_1 to the x_1x_3-plane.

Set (15) actually *coincides* with the projection after removing the origin. Indeed, take an arbitrary $(x_1, x_3) \neq (0, 0)$ satisfying (15). We have $x_1, x_3 \neq 0$, otherwise $l_1 = -2$ or $m_2 = -2$ contradicting to Lemma 2. Set $x_2 = (l_1 + 2 - l_1x_1^2)/(2x_1) = (m_2 + 2 - m_2x_3^2)/(2x_3)$. Then $P_1(x_1, x_2) = P_2(x_2, x_3) = 0$. Thus $(x_1, x_2, x_3) \in C_1$ and (x_1, x_3) belongs to the projection of C_1.

Finally, we show that (15) is an irreducible cubic curve. Eq. (15) is reduced and has degree 3, otherwise the curve is a line, hence C_1 is the intersection of a plane and cylinder, i.e., a conic. Similarly, the curve is irreducible, otherwise it contains a line, and hence C_1 contains a conic or a line. □

For the curve C_3, once it does not contain a conic, the projection to the x_1x_3-plane is given by similar equations (11)–(12), only l_1, m_1, l_2, m_2 are replaced by m_4, l_4, m_3, l_3 respectively. If the 2×2 net is deformable, then by Lemma 1 the projections of C_1 and C_3 have a common curve $(x_1(t), x_3(t))$. But both projections are irreducible, thus their reduced equations are *proportional*, i.e., the left sides become equal polynomials after multiplication by a nonzero constant. Let us study two typical possibilities for that.

Lemma 6. *Assume that C_1 does not contain a conic. Denote by* (11')–(12') *equations* (11)–(12) *with l_1, m_1, l_2, m_2 replaced by m_4, l_4, m_3, l_3 respectively. If at least one pair of equations*

(a) *(11')* and (11), *where* $m_1 \neq 0$;
(b) *(12')* and (12), *where* $m_1 = l_2 = m_3 = l_4 = 0$;

is proportional, then the 2×2 *net satisfies condition (i) of Theorem 1.*

Proof. (a) Assume that (11') equals (11) multiplied by some $\alpha \neq 0$. Comparing the coefficients at $x_1x_3^3$, x_3^4, $x_1^3x_3$, x_1^4, $x_1^2x_3^2$, x_1x_3, 1, x_3^2, x_1^2 respectively, we get the system (see [36, Section 5]):

$$l_4 l_3 = \alpha m_1 m_2 \tag{16}$$
$$l_4^2 l_3^2 = \alpha m_1^2 m_2^2 \tag{17}$$
$$m_4 m_3 = \alpha l_1 l_2 \tag{18}$$
$$m_4^2 m_3^2 = \alpha l_1^2 l_2^2 \tag{19}$$
$$l_3 m_3 l_4 m_4 - 2l_4 m_4 - 2l_3 m_3 = \alpha\Big(l_1 m_1 l_2 m_2 - 2l_1 m_1 - 2l_2 m_2\Big) \tag{20}$$
$$(2m_3 + l_3 + 2)l_4 + (m_4 + 2)m_3 = \alpha\Big((2l_2 + m_2 + 2)m_1 + (l_1 + 2)l_2\Big) \tag{21}$$
$$\Big((m_4 + 2)m_3 - l_4(l_3 + 2)\Big)^2 = \alpha\Big((l_1 + 2)l_2 - m_1(m_2 + 2)\Big)^2 \tag{22}$$
$$l_4\Big((l_3^2 + 2l_3 + 2)l_4 - (l_3 m_3 - 2)(m_4 + 2)\Big) = \alpha m_1\Big((m_2^2 + 2m_2 + 2)m_1 - (l_2 m_2 - 2)(l_1 + 2)\Big) \tag{23}$$
$$m_3\Big((m_4^2 + 2m_4 + 2)m_3 - (l_4 m_4 - 2)(l_3 + 2)\Big) = \alpha l_2\Big((l_1^2 + 2l_1 + 2)l_2 - (l_1 m_1 - 2)(m_2 + 2)\Big). \tag{24}$$

Let us prove that all the solutions of the system are given by $\alpha = 1$ and $(l_1, m_1, l_2, m_2) = (m_4, l_4, m_3, l_3)$.

First note that $l_4 \neq 0$. Indeed, otherwise (16) implies $m_2 = 0$ and (23) implies $l_1 + m_1 + 2 = 0$ which contradicts Lemma 2. Now consider two cases.

Case 1: $m_3 = 0$. Then we get $l_2 = 0$ from (18) if $l_1 \neq 0$, and from (24) if $l_1 = 0$ because of $l_2 + m_2 + 2 \neq 0$. If $\alpha \neq 1$, then using $m_1, l_4 \neq 0$, from (16)–(17) we get $m_2 = l_3 = 0$. Using $l_2, m_2, l_3, m_3 = 0$ in (21)–(22), we obtain $l_4 = \alpha m_1$ and $l_4^2 = \alpha m_1^2$ which together give $\alpha = 1$, contradiction. Therefore, $\alpha = 1$, and using $m_3 = l_2 = 0$ in (16), (20), (21), we get $l_3 l_4 = m_1 m_2$, $l_4 m_4 = l_1 m_1$, $l_4 = m_1$. These all together give $(l_1, m_1, l_2, m_2) = (m_4, l_4, m_3, l_3)$ and we are done.

Case 2: $m_3 \neq 0$. First, let us prove that $\alpha = 1$. Assume the converse. Since $m_1, l_4 \neq 0$, from (16)–(17) we get $m_2 = l_3 = 0$, and from (18)–(19) we get $l_1 l_2 = m_4 m_3 = 0$. Since $l_1 \neq 0$ by Remark 2 and $m_3 \neq 0$, we obtain $l_2 = m_4 = 0$. Then (24) becomes $m_3(l_3 + m_3 + 2) = 0$ which contradicts to Lemma 2. Thus $\alpha = 1$.

Then (16) and (18) become $l_3 l_4 = m_1 m_2$ and $l_1 l_2 = m_3 m_4$, respectively. Using the latter equations in (21), we express

$$l_2 = \frac{(m_3 + 1)(l_4 + 1)}{m_1 + 1} - 1, \quad l_3 = \frac{m_1 m_2}{l_4},$$

$$m_4 = \frac{l_1 l_2}{m_3} = \frac{l_1(m_3 l_4 + m_3 + l_4 - m_1)}{m_3(m_1+1)}. \tag{25}$$

Substituting (25) into (22) and (23), we get (see [36, Section 6])

$$\begin{aligned}
&(m_1+m_3+2)(l_4-m_1)\cdot\\
&\quad\cdot\Big(\underbrace{(m_3+1)(l_1+1)(l_4+1)-(m_1+1)(m_1m_2+l_1+l_4+m_1-m_3+1)}_{A}\Big)=0,\\
&(l_4-m_1)\Big(A+(1+m_3)m_1\underbrace{(m_1m_2+m_2m_3+l_1+m_2+l_4+m_1+2)}_{B}\Big)=0.
\end{aligned}$$

Now if $l_4 \neq m_1$, then $A = B = 0$ because $m_1, m_1+m_3+2, 1+m_3 \neq 0$ by Lemma 2. Then $A+(m_1-m_3)B = (1+m_3)(l_1l_4-m_2m_3) = 0$ (see [36, Section 7]), thus $l_1l_4 = m_2m_3$. Hence $B = (m_1+1)(m_2+1)+(l_1+1)(l_4+1) = 0$ which contradicts to Lemma 2.

Therefore, $l_4 = m_1$, and from (25) we get $(l_1, m_1, l_2, m_2) = (m_4, l_4, m_3, l_3)$ and we are done.

(b) If the coefficients of (12') and (12) are proportional, then $m_4 = l_1$ and $l_3 = m_2$. Since $m_1 = l_2 = m_3 = l_4 = 0$, by Lemma 2(i) we arrive at condition (i). □

Finally, we summarize the whole argument.

Proof of Theorem 1. Conditions (i)–(ii) are sufficient by Example 2. Let us prove that they are necessary. Assume that the 2×2 net is deformable. Then by Lemma 1 system (6) has a continuous family of real solutions $\big(x_1(t), x_2(t), x_3(t), x_4(t)\big)$ with all $x_i(0) = 1$. Recall that C_i denotes the curve given by $P_i(x_i, x_{i+1}) = P_{i+1}(x_{i+1}, x_{i+2}) = 0$, where the indices are cyclic modulo 4.

Case (ii): *each curve $C_1, \dots, C_4$ contains a conic.* Then the theorem follows from Corollary 2.

Case (i): *at least one of the curves $C_1, \dots, C_4$ does not contain a conic.* We use a symmetry argument to minimize the number of subcases below: First, assume without loss of generality that C_1 does not contain a conic. Second, assume that m_1 has the maximal absolute value among all m_i and l_{i+1} such that C_i does not contain a conic (otherwise perform either a suitable cyclic permutation of variables $x_1, \dots, x_4$ or reverse their order).

The projections of C_1 and C_3 to the x_1x_3-plane have a common curve $\big(x_1(t), x_3(t)\big)$. By Lemma 5, the projection of C_1 is an irreducible curve of degree 3 or 4. Thus the curve C_3 of degree at most 4 cannot contain a conic, otherwise both C_3 and its projection split into a union of conics and/or lines, not curves of higher degree. So, by Lemma 5 the projections of C_1 and C_3 are irreducible curves given by (11) or (12), with l_1, m_1, l_2, m_2 replaced by m_4, l_4, m_3, l_3 respectively in case of C_3. Since both projections are irreducible, their reduced equations must be proportional. Consider 2 subcases.

Subcase (a): $m_1 \neq 0$. In this case, the two projections are given by (11) and (11'): they cannot be given by (11) and (12') because the degrees are equal. By Lemma 6(a), the theorem follows.

Subcase (b): $m_1 = 0$. Recall that m_1 was chosen to have the maximal absolute value among all m_i and l_{i+1} such that C_i does not contain a conic. Thus $|l_2|, |m_3|, |l_4| \leq |m_1| = 0$ and hence $l_2 = m_3 = l_4 = 0$. By Lemma 6(b), the theorem follows. □

Remark 4. In our setup, the so-called *Stachel conjecture* holds: the resultant of at least one consecutive pair of homogenized polynomials $P_i(x_i, x_{i+1})$, where $i = 1, 2, 3, 4$, is reducible. Indeed, by Theorem 1, at least one pair of adjacent faces f_i, f_{i+1} has equal opposite ratios with respect to their common edge. By Lemma 3, the curve C_i, hence its projection to the $x_i x_{i+2}$-plane, contains a conic or a line. Hence the resultant of P_i and P_{i+1} has a factor of degree 2 or 1. But the resultant itself, when homogenized, has always degree 3 or 4; see (11)–(12). Thus it is reducible. The example of a 2×2 net with all the faces being parallelograms shows that the homogenization of the polynomials is necessary here.

3. Deformable $m \times n$ Nets

In this section, we characterize all deformable nets of arbitrary size. We state the classification in Sect. 3.1, discuss the geometry of deformable nets in Sect. 3.2, and give the proof in Sect. 3.3.

3.1. Statement of the Classification

We need the following notions. By an $a \times b$ *sub-net* of a given $m \times n$ net with the points P_{ij}, where $0 \leq i \leq m$ and $0 \leq j \leq n$, we mean an $a \times b$ net with the points P_{ij}, where $p \leq i \leq p + a$ and $q \leq j \leq q + b$, for some integers $0 \leq p \leq n - a$ and $0 \leq q \leq m - b$. (The collection of $(a + 1)(b + 1)$ points indexed in this way is still viewed as an $a \times b$ net.) In particular, a 1×2 sub-net is formed by two faces with a common edge on a parameter line $j = \text{const}$, and a 2×1 sub-net is formed by two faces with a common edge on a parameter line $i = \text{const}$.

Theorem 9. *An $m \times n$ net is deformable if and only if one of the following conditions holds:*

(i) *in each 1×2 sub-net or in each 2×1 sub-net, the two faces are affine symmetric with respect to their common edge;*
(ii) *each pair of faces with a common edge has equal opposite ratios with respect to that edge.*

Thus all the 2×2 sub-nets of a deformable $m \times n$ net belong to the same class, (i) or (ii).

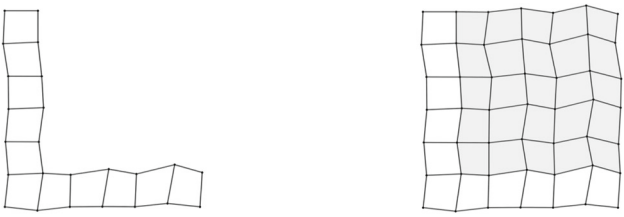

FIGURE 13. Left: An L-shaped net of size 6×6. Right: The unique deformable 6×6 net containing the L-shaped net. See Corollary 3

Theorem 9 allows us to check if a given net is deformable. Now we give a parametrization of deformable nets, allowing us to construct all deformable nets close enough to a square net.

By an *L-shaped net of size* $m \times n$ we mean an indexed collection of $2m+2n$ points P_{ij}, where the indices satisfy the inequalities $0 \leq i \leq m$, $0 \leq j \leq n$, $\min\{i, j\} \leq 1$, such that $P_{ij}, P_{i+1,j}, P_{i,j+1}, P_{i+1,j+1}$ are consecutive vertices of a convex quadrilateral whenever $i = 0$, $0 \leq j < n$ or $j = 0$, $0 \leq i < m$. See Fig. 13. *Edges*, *faces*, and *sub-nets* are defined analogously to the ones of an $m \times n$ net. An *L-shaped square net* is an L-shaped net such that all the faces are coplanar non-coincident squares.

Corollary 3. *If an L-shaped net of size* $m \times n$ *is sufficiently close to the L-shaped square net and satisfies one of conditions (i) or (ii) in Theorem 9, then it is contained in exactly one deformable* $m \times n$ *net.*

Moreover, the resulting $m \times n$ *net continuously depends on the given L-shaped net.*

The reader interested in the proofs of the theorem and the corollary can proceed to Sect. 3.3, and now we discuss geometric properties of the resulting classes (i) and (ii) of deformable $m \times n$ nets.

3.2. Geometric Properties

3.2.1. Class (i). Deformable nets from class (i) are related to cone nets, which are studied in [26].

An $1 \times n$ net with points P_{ij}, where $0 \leq i \leq 1$, $0 \leq j \leq n$, is called a *cone strip* if all the lines $P_{0j}P_{1j}$ for $0 \leq j \leq n$ are either concurrent or parallel. See Fig. 14(left). An $m \times n$ net is called a *cone net* if each $1 \times n$ or each $m \times 1$ sub-net is a cone strip. See Fig. 15. Applying Proposition 2 repeatedly (see the red lines in Fig. 7), we see that each net from class (i) is a cone net.

The other condition depicted in Fig. 7 leads us to the following notions. By *a cone-cylinder strip* we mean a cone strip such that $P_{0,j}P_{0,j+1} \parallel P_{1,j}P_{1,j+1}$ for each $0 \leq j \leq n-1$. See Fig. 14(middle). A *doubled cone-cylinder strip* is a cone strip such that $P_{0,j}P_{0,j+2} \parallel P_{1,j}P_{1,j+2}$ and $P_{0,j}, P_{0,j+2}, P_{1,j}, P_{1,j+2}$ are

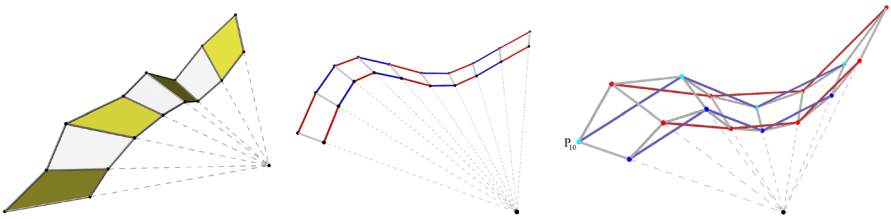

FIGURE 14. Left: a cone strip. Middle: a cone-cylinder strip. Right: a doubled cone-cylinder strip. Corresponding blue (red) segments are parallel, and the dashed lines are concurrent. The doubled cone-cylinder strip consists of two interleaved cone-cylinder strips shown in red and shades of blue respectively. Given the red strip, one can construct the blue one so that they form a doubled cone-cylinder strip together: the dark blue points can be chosen (almost) arbitrarily, the point P_{10} can be freely chosen on the dashed line, and the remaining light blue points are determined by the parallelism of the resulting blue segments. The construction can then be propagated to the next strips in a net

non-collinear for each $0 \le j \le n-2$. See Fig. 14(right). We see that a doubled cone-cylinder strip consists of two interleaved cone-cylinder strips forming a cone strip together. A *cone-cylinder net* and a *doubled cone-cylinder net* are now defined analogously to a cone net. See Fig. 15. The faces of a cone-cylinder net are trapezoids, but those are not T-nets of [37] because the parameter lines need not be planar. The points $P_{00}, P_{0n}, P_{m0}, P_{mn}$ are called the *corners* of an $m \times n$ net.

As an immediate consequence of Proposition 2, we get a geometric characterization of class (i).

Proposition 10. *An $m \times n$ net such that the corners of each 2×1 and 1×2 sub-net are non-collinear satisfies condition (i) of* Theorem 9 *if and only if it is a doubled cone-cylinder net.*

We see that any $m \times n$ net from class (i) consists of two cone-cylinder nets forming a cone net together. Given one of the two cone-cylinder nets, one can construct the other one so that they comprise a net from class (i) together. See Fig. 14(right).

This suggests taking a closer look at the cone-cylinder nets. They have applications themselves [27].

Proposition 11. *An $m \times n$ net with the points P_{ij}, where $0 \le i \le m$, $0 \le j \le n$, is a cone-cylinder net if and only if up to interchanging the indices i and j we have*

$$P_{ij} = a_i + \sigma_i b_j, \qquad 0 \le i \le m \text{ and } 0 \le j \le n, \tag{26}$$

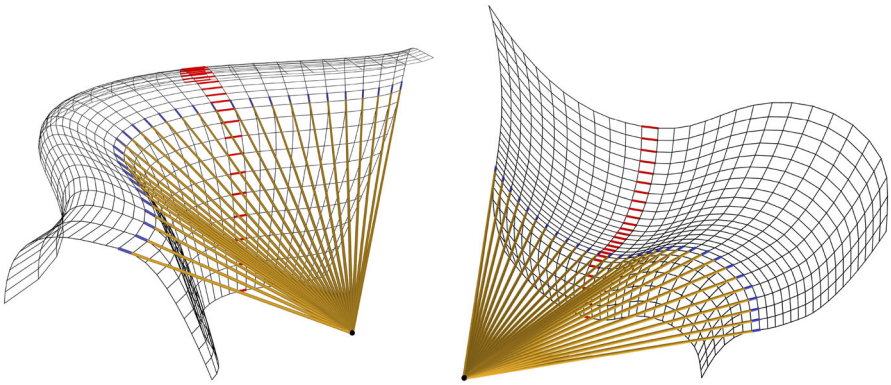

FIGURE 15. Cone-cylinder nets. Left: the deformable net from Fig. 1. Right: another example. The yellow lines are concurrent and the red lines are parallel

for some $a_0, \dots, a_m, b_0, \dots, b_n \in \mathbb{R}^d$ *and* $\sigma_0, \dots, \sigma_m \in \mathbb{R}$.

Proof. The 'only if' part. Take a cone-cylinder net. Up to interchanging the indices i and j, we may assume that all $1 \times n$ sub-nets are cone-cylinder strips. Then for each $0 \le i < m$, the broken line $P_{i+1,0} \dots P_{i+1,n}$ is obtained from $P_{i,0} \dots P_{i,n}$ by a central similarity or a translation. Then all the broken lines are obtained from $P_{0,0} \dots P_{0,n}$ by central similarities or translations. This means that (26) holds for $b_j := P_{0,j}$ and suitable a_i and σ_i.

The 'if' part. Take an $m \times n$ net given by (26). Any broken line $P_{i,0} \dots P_{i,n}$ (with constant i) arises from the broken line $b_0 \dots b_n$ by uniform scaling with factor σ_i and subsequent translation by a_i. Hence, two consecutive broken lines $P_{i,0} \dots P_{i,n}$ and $P_{i+1,0} \dots P_{i+1,n}$ are related by a central similarity or a translation in case of $\sigma_i = \sigma_{i+1}$. Thus, the broken lines have parallel edges and are connected by a cone, whose vertex c_i is easily seen to be

$$c_i = \frac{\sigma_{i+1} a_i - \sigma_i a_{i+1}}{\sigma_{i+1} - \sigma_i}.$$

The cone becomes a cylinder with ruling direction $a_i - a_{i+1}$ for $\sigma_i = \sigma_{i+1}$. We get a cone-cylinder net. □

As a corollary, any cone-cylinder net (at least, with noncoplanar faces) is also a doubled cone-cylinder net, hence is deformable. One can also construct the deformation explicitly. This will be a special case of a *conical Combescure transform* from [26, §4]. We assume $\sigma_i > 0$ for simplicity.

Proposition 12. *A cone-cylinder net* (26) *with all* $\sigma_i > 0$ *is embedded into a family*

$$P_{ij}(t) := \underbrace{a_0 + \sum_{k=1}^{i} \frac{(a_k - a_{k-1})\,(\sigma_k + \sigma_{k-1})}{\sqrt{t+\sigma_k^2} + \sqrt{t+\sigma_{k-1}^2}}}_{a_i(t)} + \underbrace{\sqrt{t+\sigma_i^2}}_{\sigma_i(t)}\, b_j,\ 0 \le i \le m, 0 \le j \le n, \quad (27)$$

of cone-cylinder nets, which are its area-preserving Combescure transformations, for some $\varepsilon > 0$ *and all* $t \in [0, \varepsilon]$.

Proof. By Proposition 11, net (27) is a cone-cylinder net for each t sufficiently close to 0, because it is of the form $P_{ij}(t) = a_i(t) + \sigma_i(t) b_j$. For $t = 0$, it coincides with (26) because all $\sigma_i > 0$. Since

$$\begin{aligned}
\overrightarrow{P_{i,j-1}(t)P_{ij}(t)} &= \sqrt{t+\sigma_i^2} \cdot (b_j - b_{j-1}) = \frac{\sqrt{t+\sigma_i^2}}{\sigma_i} \cdot \overrightarrow{P_{i,j-1}P_{ij}},\\
\overrightarrow{P_{i-1,j}(t)P_{ij}(t)} &= \frac{(a_i - a_{i-1})\,(\sigma_i + \sigma_{i-1})}{\sqrt{t+\sigma_i^2} + \sqrt{t+\sigma_{i-1}^2}} + \left(\sqrt{t+\sigma_i^2} - \sqrt{t+\sigma_{i-1}^2}\right) b_j\\
&= \frac{(\sigma_i + \sigma_{i-1})\overrightarrow{P_{i-1,j}P_{ij}}}{\sqrt{t+\sigma_i^2} + \sqrt{t+\sigma_{i-1}^2}}
\end{aligned}$$

for each $t \in [0, \varepsilon]$, nets (27) and (26) are Combescure transforms. Area preservation follows from

$$\begin{aligned}
&(P_{i,j-1}(t)P_{ij}(t) + P_{i-1,j-1}(t)P_{i-1,j}(t)) \cdot P_{i-1,j}(t)P_{ij}(t) =\\
&\quad = |b_j - b_{j-1}|(\sigma_i + \sigma_{i-1})P_{i-1,j}P_{ij} = \text{const}.
\end{aligned}$$

For distinct $t \in [0, \varepsilon]$, nets (27) are non-congruent because the edge lengths $P_{i,j-1}(t)P_{ij}(t)$ are distinct. □

3.2.2. Class (ii). All we said about 2×2 nets from class (ii) in Sect. 2.2 remains true for $m \times n$ nets. Propositions 4, 5, 7 remain true with the same proofs, if "2×2" is replaced by "$m \times n$" (because an $m \times n$ net is a Kœnigs net if and only if all its 2×2 sub-nets are):

Proposition 13. *An* $m \times n$ *net satisfies condition (ii) of* Theorem 9 *if and only if it has a Christoffel dual with the same areas of corresponding faces. For such an* $m \times n$ *net, a family of area-preserving Combesure transformations is given by* (3) *for* $0 \le i \le m$ *and* $0 \le j \le n$.

Corollary 4. *A deformable* $m \times n$ *net has a deformable Christoffel dual.*

Proof. By Theorem 9, a deformable $m \times n$ net belongs to one of the classes (i)–(ii). For class (ii), the desired result follows from Proposition 13 immediately. For class (i), we construct the deformable Christoffel dual as follows. Assume that each 1×2 sub-net is *affine symmetric*, that is, its two faces are affine symmetric with respect to their common edge, hence have equal opposite ratios

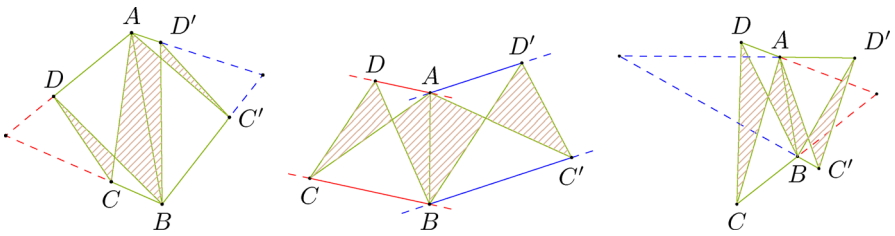

FIGURE 16. The position of the intersection points of the opposite sides of quadrilaterals $ABCD$ and $ABC'D'$ having equal opposite ratios with respect to the common side AB

with respect to corresponding edges. Then, each $1 \times n$ sub-net belongs to class (ii) as well, and by Proposition 13, it has a Christoffel dual $1 \times n$ net with the same areas of corresponding faces. By Proposition 6, the opposite ratio of a face f with respect to an edge e is inverse to the opposite ratio of the dual face f^* with respect to e^*. Thus the Christoffel dual $1 \times n$ nets still have affine symmetric 1×2 sub-nets and can be scaled to compose the whole Christoffel dual $m \times n$ net altogether. The latter still belongs to class (i) and hence is deformable. □

In class (ii), the following *zig-zag phenomenon* occurs. Recall that by Proposition 8 the rays extending the sides BC and AD of a convex quadrilateral $ABCD$ intersect if and only if the opposite ratio of $ABCD$ with respect to AB is greater than 1. If two quadrilaterals $ABCD$ and $ABC'D'$ in the plane have a common side AB (and no other common points), and opposite ratios with respect to that side are equal, then the pairs of lines BC, AD and BC', AD' intersect on the opposite sides of the line AB, unless $BC \parallel AD$ and $BC' \parallel AD'$. See Fig. 16. For spatial nets from class (ii), the same happens in the projection to any plane. This shows that the 'zig-zag' shape of the discrete parameter lines like in Fig. 3 is unavoidable unless the parameter lines have parallel edges. The same is true for class (i), but only for the parameter lines in one of the two directions. Cf. [26, Figure 5 to the right].

3.3. Proof of the Classification

For the proof of the classification of deformable $m \times n$ nets, we need the following lemmas describing deformations of their small sub-nets.

Lemma 7. *For each segment e' parallel and sufficiently close in length to an edge e of a 1×1 net, there exists a unique deformation of this net such that e' is its edge corresponding to e.*

Proof. Denote by $ABCD$ the only face of the 1×1 net with $AB := e$. Let A', B' be the endpoints of the segment e' so that $\overrightarrow{AB}$ and $\overrightarrow{A'B'}$ have the same direction. Consider arbitrary points C', D' on the two rays cooriented with

BC, AD starting at B', A', respectively, such that $\overrightarrow{C'D'}$ and $\overrightarrow{CD}$ have the same direction. Since e' has a sufficiently close length to e, we may continuously move the segment $C'D'$ so that it remains parallel to CD, the quadrilateral $A'B'C'D'$ remains convex, and the area of $A'B'C'D'$ changes monotonically and continuously in an interval containing the value of the area of $ABCD$. Therefore, we can choose positions of C', D' so that the quadrilaterals $ABCD$ and $A'B'C'D'$ have the same areas. The resulting quadrilateral $A'B'C'D'$ is the desired unique deformation. (Indeed, it is contained in a continuous family of parallel 1×1 nets of the same area, obtained by the same construction for some continuous family of segments between e and e'. Conversely, any deformation of $ABCD$ is contained in a continuous family, hence it has the same edge directions, hence coincides with $A'B'C'D'$ above and is unique.) □

Lemma 8. *For each segment e' parallel and sufficiently close in length to an edge e of a deformable 2×2 net, there is a unique deformation of the net such that e' is its edge corresponding to e.*

Proof. Uniqueness. Consider a deformation of the 2×2 net such that e' is its edge corresponding to e. By Lemma 7, each 1×1 sub-net containing the edge e' is determined uniquely. This means that the faces containing e' and all the edges of those faces are determined uniquely. Applying Lemma 7 to the adjacent faces repeatedly, we get that they all are determined uniquely.

Existence. By Theorem 1, a deformable 2×2 net satisfies one of the conditions (i)–(ii) in that theorem. Take a particular family of deformations given by Example 2.

Consider the ratio of the lengths of e and its corresponding edge in a net from this family. By the 'moreover' part of Example 2, such ratios form an interval containing 1 in its interior. Since e' is close enough in length to e, there is a net in this family that the edge corresponding to e has the same length as e'. □

The 'if' part in Theorem 9 follows from Theorem 1 and the following lemma.

Lemma 9. *If each 2×2 sub-net of an $m \times n$ net is deformable, then the net is deformable.*

Proof. Let us construct the desired deformation by slightly moving vertices P_{ij} to new positions $P_{ij}(t)$, where $0 \le i \le m$ and $0 \le j \le n$, one by one.

First, let us define inductively the points $P_{ij}(t)$ for $i = 0, 1$ and $j = 0, \dots, n$. Let $P_{00}(t)$ and $P_{10}(t)$ be any points such that the edges $P_{00}(t)$ $P_{10}(t)$ and $P_{00}(0)P_{10}(0) = P_{00}P_{10}$ are parallel and have sufficiently close lengths (and continuously depend on t but are not congruent for $t \neq 0$). Now, assume that the points $P_{0j}(t)$ and $P_{1j}(t)$, where $0 \le j \le n-1$ have already been

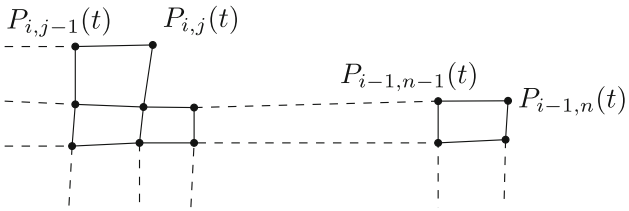

FIGURE 17. Construction of a deformation layer by layer; see the proof of Lemma 9

defined. Then by Lemma 7 there exist unique points $P_{0,j+1}(t)$ and $P_{1,j+1}(t)$ such that the quadrilaterals $P_{0,j}P_{0,j+1}P_{1,j+1}P_{1,j}$ and $P_{0,j}(t)P_{0,j+1}(t)P_{1,j+1}(t)P_{1,j}(t)$ have parallel sides, equal areas, and depend on t continuously. By induction, we define $P_{ij}(t)$ for $i = 0, 1$ and all $j = 0, \dots, n$.

For $m = 1$ (and similarly for $n = 1$), this finishes the proof. Assume $m, n \geq 2$. Now we define the points $P_{ij}(t)$ inductively for $i = 2, \dots, m$ and $j = 0, \dots, n$. See Fig. 17.

Assume that for some $1 \leq k \leq n-1$ the points $P_{ij}(t)$, where $0 \leq i \leq k-1$ and $j = 0, \dots, n$ have already been defined. Let us define the points $P_{ij}(t)$ for $i = k$ and $j = 0, \dots, n$.

Apply Lemma 8 to the 2×2 sub-net formed by the vertices P_{ij}, where $k-2 \leq i \leq k$ and $0 \leq j \leq 2$, the edges $e' = P_{k-1,0}(t)P_{k-1,1}(t)$ and $e = P_{k-1,0}P_{k-1,1}$. The latter edges are indeed parallel and have close lengths by construction. Consider the deformation $P_{ij}(t)$, where $k-2 \leq i \leq k$ and $0 \leq j \leq 2$, of the 2×2 sub-net given by the lemma. Then the vertices $P_{k,0}(t), P_{k,1}(t), P_{k,2}(t)$ are the desired ones. Note that the positions of the vertices $P_{k-1,2}(t), P_{k-2,0}(t), P_{k-2,1}(t), P_{k-2,2}(t)$ in the deformation of the 2×2 sub-net coincide with the ones constructed before because of Lemma 7.

Finally, assume that the points $P_{k,0}(t), \dots, P_{k,l}(t)$ have already been defined for some $2 \leq l \leq n-1$. Let us define the point $P_{k,l+1}(t)$. Apply Lemma 8 to the 2×2 sub-net formed by the vertices P_{ij}, where $k-2 \leq i \leq k$ and $l-1 \leq j \leq l+1$, the edges $e' = P_{k-1,l-1}(t)P_{k-1,l}(t)$ and $e = P_{k-1,l-1}P_{k-1,l}$. The resulting deformation of the 2×2 sub-net gives the desired point $P_{k,l+1}(t)$. Note that the positions of the other vertices in the deformation of the sub-net coincide with the ones constructed before because of Lemma 7. Now the lemma follows by induction. □

Remark 5. Note that this lemma was not simple at all: to "propagate" a deformation to all 2×2 sub-nets, we needed to ensure that *for any edge, a* 2×2 *sub-net has both a deformation increasing its length and a deformation decreasing it* (the 'moreover' part of Example 2). We do not know how to prove this without proving the whole Classification Theorem 1.

The same concerns flexible nets in Euclidean geometry [33, Theorem 3.2]: to "propagate" a deformation to all 3×3 sub-nets, we need to ensure that *for*

any edge, a 3×3*sub-net has both a flexion increasing the dihedral angle at the edge and a flexion decreasing it.* Otherwise, a priori, one flexible 3×3 sub-net of a 3×4 net could have no flexions increasing a particular dihedral angle, and the other flexible 3×3 sub-net could have no flexions decreasing it; thus, the whole 3×4 net would not be flexible. This has been overlooked before, although a similar phenomenon occurs in the smooth setup; see, e.g., [37, Figure 18]. We conjecture that the analog of Lemma 9 for Euclidean flexible nets is *not* true. This shows again that the isotropic analog of a Euclidean problem gives insight into the latter.

For the 'only if' part of Theorem 9, we need the following construction and lemmas.

To an $m \times n$ net P_{ij}, assign two $m \times n$ tables H and V filled by real numbers as follows. The cells of the tables are in the obvious bijection with the faces of the net. We fill the cells (faces) as follows.

Into a face $P_{ij}P_{i-1,j}P_{i-1,j-1}P_{i,j-1}$ of the table H, where $1 \le i \le m$ and $1 \le j \le n$, put the opposite ratio of the face with respect to the side $P_{ij}P_{i,j-1}$ (respectively, $P_{i-1,j}P_{i-1,j-1}$) if i is even (respectively, odd). Into the same face of the table V, put the opposite ratio with respect to the side $P_{ij}P_{i-1,j}$ (respectively, $P_{i,j-1}P_{i-1,j-1}$) if j is even (respectively, odd).

Clearly, conditions (i)–(ii) of Theorem 9 can then be restated as follows.

Lemma 10. *Conditions (i)–(ii) of* Theorem 9 *are equivalent to the following ones:*

(i) *both tables* H *and* V *have equal rows or both have equal columns;*
(ii) *table* H *has equal rows and table* V *has equal columns.*

For a deformable 2×2 net, one of the resulting conditions holds by Theorem 1. The same concerns 2×2 sub-nets of a deformable $m \times n$ net. We come to the following simple lemma.

Lemma 11. *An* $m \times n$ *table is filled by real numbers. Assume that each square* 2×2 *consists of two equal rows or two equal columns. Then all rows or all columns of the table are equal.*

Proof. Assume that $m, n \ge 2$; otherwise there is nothing to prove. We prove the lemma by induction on $m+n$. The induction base, $m+n = 4$, i.e., $m = n = 2$, is automatic. To perform the induction step, assume that $m + n \ge 5$ and the lemma holds for any $(m-1) \times n$ or $m \times (n-1)$ table, and let us prove it for an $m \times n$ table. Consider the following two cases:

Case 1: some two neighboring non-corner cells of the $m \times n$ table contain unequal numbers. Without loss of generality, the two cells belong to one row. They are both contained in two different $(m-1) \times n$ tables or two different $m \times (n-1)$ tables. Then by the inductive hypothesis, each of the two tables has equal rows or equal columns. Since the two cells belong to one row and contain different numbers, it follows that the rows are equal. Since the two

tables have either a common row or a common column, the rows in the whole $m \times n$ table are equal as well.

Case 2: any two neighboring non-corner cells contain equal numbers. Then consider a 2×2 corner table. If $m, n \geq 3$, then the numbers in its cells must be equal, leading to the table with equal numbers. If, say, $m = 2$, then the 2×2 table has equal rows, leading to equal rows of the $m \times n$ table. □

Let us summarize the argument.

Proof of Theorem 9. The 'if' part follows from Theorem 1 and Lemma 9. The 'only if' part follows from Theorem 1 and Lemmas 10–11. □

Proof of Corollary 3. Given the first row and the first column of tables H and V, any of conditions (i)–(ii) in Lemma 10 uniquely determines all the other entries. By Theorem 9, this means that the L-shaped $m \times n$ net uniquely determines the opposite ratios of all the other faces of the desired deformable $m \times n$ net. It remains to show that those faces are uniquely determined by their opposite ratios.

We define inductively the points P_{ij} where $2 \leq i \leq m$, $2 \leq j \leq n$, repeatedly applying Corollary 1 to all faces; see Fig. 17. Assume that the points $P_{i-1,j-1}$, $P_{i-1,j}$, $P_{i,j-1}$ have already been determined. The points are not collinear if the L-shaped $m \times n$ net is close to the L-shaped square net. By Corollary 1, there is a unique point P_{ij} such that $P_{i-1,j-1}P_{i-1,j}P_{ij}P_{i,j-1}$ has the desired opposite ratios with respect to $P_{i-1,j-1}P_{i-1,j}$ and $P_{i-1,j-1}P_{i,j-1}$. By induction, the corollary follows. □

4. Smooth Deformable Nets

In the previous section, we described all deformable discrete nets. We now proceed to smooth deformable nets and do this only by finding the smooth analogs of the above classes.

4.1. Cone-Cylinder Nets

Discrete deformable nets of class (i) are combinations of two interleaved discrete cone-cylinder nets. The smooth analog of both must be the same smooth surface. Passing from the discrete variables i and j to continuous variables u and v in (26), we conclude that the smooth analog of class (i) is exactly the *smooth cone-cylinder nets*, that is, the ones that possess a parameterization of the form

$$f(u, v) = a(u) + \sigma(u)b(v), \quad (u, v) \in U = [\alpha, \beta] \times [\gamma, \delta] \subset \mathbb{R}^2, \tag{28}$$

for some smooth functions $a\colon [\alpha, \beta] \to \mathbb{R}^d$, $b\colon [\gamma, \delta] \to \mathbb{R}^d$, $\sigma\colon [\alpha, \beta] \to \mathbb{R}$. These surfaces have been used in architectural design [27], where they are called *scale-translational surfaces* with base curves $a(u)$ and $b(v)$ and scaling function $\sigma(u)$. Indeed, curve $b(v)$ gets scaled with $\sigma(u)$. Without scaling ($\sigma(u) = 1$), one obtains ordinary translational surfaces.

In the following, we assume a parameter rectangle $U = [\alpha, \beta] \times [\gamma, \delta] \subset \mathbb{R}^2$ on which parameterizations $f(u, v)$ are regular. This means that $f_u(u, v) \nparallel f_v(u, v)$ for each $(u, v) \in U$ or, in our case, $a'(u) + \sigma'(u)b(v) \nparallel \sigma(u)b'(v)$. In particular, $\sigma(u) \neq 0$ everywhere. Assume without loss of generality that $\sigma(u) > 0$; otherwise, change the sign of both σ and b. We see that $f(u, v)$ is a *conjugate net*, which means that the mixed partial derivative f_{uv} at each point is parallel to the tangent plane; here $f_{uv} = \sigma'(u)b'(v)$ is even parallel to $f_v = \sigma(u)b'(v)$.

Proposition 14. *A conjugate net $f\colon U \to \mathbb{R}^d$ has form (28) with $\sigma(u) > 0$ if and only if the tangents to the u-parameter lines at points of each v-parameter line are concurrent or parallel and the tangents to the v-parameter lines at points of each u-parameter line are parallel.*

Proof. Since f is a conjugate net, it follows that $f_{uv} = pf_u + qf_v$ for some $p, q\colon U \to \mathbb{R}$. Then [26, Lemma 2] asserts that the conditions on the u- and v-parameter lines in the proposition are equivalent to $pq = q_v$ and $p = 0$, respectively. Those are satisfied for net (28) because it has $f_{uv} = f_v\sigma'(u)/\sigma(u)$.

Conversely, if $pq = q_v$ and $p = 0$, then $q = q(u)$ does not depend on v. We get $f_{uv} = q(u)f_v$. Integrating with respect to v, we get $f_u = q(u)f + c(u)$ for some function $c\colon [\alpha, \beta] \to \mathbb{R}^d$. Let $\sigma\colon [\alpha, \beta] \to \mathbb{R}$ be any positive solution of $\sigma'/\sigma = q$. Then we can write the equation $f_u = q(u)f + c(u)$ in the form $(f/\sigma)'_u = c/\sigma$. Again, integrating with respect to u and multiplying both sides by σ, we arrive at $f(u, v) = a(u) + \sigma(u) \cdot b(v)$ for some $a\colon [\alpha, \beta] \to \mathbb{R}^d$ and $b\colon [\gamma, \delta] \to \mathbb{R}^d$. □

We found more than just the fact that $f(u, v)$ in equation (28) represents a smooth cone-cylinder net. We see that *sampling the parameter intervals for $a(u)$ and $b(v)$ and evaluating $f(u, v)$ on the resulting grid yields a discrete $m \times n$ cone-cylinder net*. We have here an instant of a multi-Q-net in the sense of Bobenko et al. [28].

We now proceed to deformations (area-preserving C-trafos) of surfaces (28) and provide an analytical proof of deformability.

Two conjugate nets $f, f^+\colon U \to \mathbb{R}^d$ are *parallel* or *Combescure transforms* of each other if $f_u(u, v) \parallel f^+_u(u, v)$ and $f_v(u, v) \parallel f^+_v(u, v)$ for each $(u, v) \in U$. A Combescure transform f^+ of a conjugate net f is *area-preserving*, if determinants of the first fundamental forms agree,

$$\langle f_u, f_u\rangle \cdot \langle f_v, f_v\rangle - \langle f_u, f_v\rangle^2 = \langle f^+_u, f^+_u\rangle \cdot \langle f^+_v, f^+_v\rangle - \langle f^+_u, f^+_v\rangle^2,$$

at each point $(u, v) \in U$, where $\langle x, y\rangle$ denotes the scalar product of vectors x and y. Two conjugate nets $f, f^+\colon U \to \mathbb{R}^d$ are *congruent*, if $f^+ = g \circ f$ for some isometry $g\colon \mathbb{R}^d \to \mathbb{R}^d$.

A conjugate net $f(u, v)$ is called *deformable* if it belongs to a continuous family of pairwise non-congruent area-preserving Combescure transforms $f^+(u, v, t)$, where $t \in [0, 1]$.

It would be interesting to find all smooth deformable nets. We have the following partial result.

Proposition 15. *Any regular cone-cylinder net* (28) *is deformable. For* $\sigma(u) > 0$*, it is embedded into a one-parameter family*

$$f^+(u,v,t) := \underbrace{a(\alpha) + \int_\alpha^u \frac{a'(w)\sigma(w)\,dw}{\sqrt{t+\sigma(w)^2}}}_{a(u,t)} + \underbrace{\sqrt{t+\sigma(u)^2}}_{\sigma(u,t)} b(v), \quad t \in [0,1],\ (u,v) \in U, \tag{29}$$

of cone-cylinder nets which are related to each other by area-preserving Combescure transformations.

This is a particular case of a *conical Combescure transformation* introduced in [26, Definition 4].

Proof. To prove that f is deformable, the continuous family (29) has to consist of non-congruent area-preserving Combescure transforms $f^+\colon U \times [0,1] \to \mathbb{R}^d$.

Since $f^+(u,v,0) = f(u,v)$, the family f^+ contains f. Clearly, $f^+(u,v,t)$ is continuous.

Since

$$\sigma \cdot b' = f_v(u,v) \parallel f_v^+(u,v,t) = \sqrt{t+\sigma^2} \cdot b' \quad \text{and}$$
$$a' + \sigma' b = f_u(u,v) \parallel f_u^+(u,v,t) = \frac{\sigma(a'+\sigma' b)}{\sqrt{t+\sigma^2}},$$

for each $t \in [0,1]$ and $(u,v) \in U$, the nets f and f^+ are Combescure transforms. In particular, $f^+(u,v,t)$ is regular for each $t \in [0,1]$. It is a cone-cylinder net for each $t \in [0,1]$ because it is of the form $f^+(u,v,t) = a(u,t) + \sigma(u,t)b(v)$. Area preservation follows from

$$\langle f_u^+, f_u^+\rangle\langle f_v^+, f_v^+\rangle - \langle f_u^+, f_v^+\rangle^2 = \sigma^2(\|a'+\sigma' b\|^2\ \|b'\|^2 - \langle b', a'+\sigma' b\rangle^2) =$$
$$= \langle f_u, f_u\rangle\langle f_v, f_v\rangle - \langle f_u, f_v\rangle^2.$$

For distinct $t \in [0,1]$, the nets $f^+(u,v,t)$ are non-congruent because $f_v^+ = \sqrt{t+\sigma^2} \cdot b'$ are distinct by the regularity condition $b' \neq 0$. □

As for discrete deformable nets of class (ii), they do not lead to new smooth examples. Their smooth analog is smooth nets having an area-preserving Chrostoffel dual. Those are translational nets, a particular case of (28) with $\sigma(u) = 1$. Indeed, recall that a *Christoffel dual* $f^*\colon U \to \mathbb{R}^d$ of a smooth net $f\colon U \to \mathbb{R}^d$ is defined by the conditions $f_u^* = f_u/\nu^2$ and $f_v^* = -f_v/\nu^2$ for some smooth function $\nu\colon U \to (0,+\infty)$. The transform f^* is area-preserving if and only if $\nu = 1$. We get $(f+f^*)'_v = 0$, $(f-f^*)'_u = 0$, and arrive at (28) with $\sigma(u) = 1$.

Remark 6. Area-preserving Combescure transforms of smooth nets preserve the Gaussian curvature, the isotopic Gaussian curvature, and, more generally, the relative Gaussian curvature with respect to any relative sphere. Indeed, since the directions of the tangent planes are preserved, it follows that the Gaussian image is preserved, hence its area. The area of the deforming surface does not change as well. The Gaussian curvature is a limit of the ratio of these areas and is thus preserved.

4.2. Principal Cone-Cylinder Nets

Let us give a classification of smooth *principal* (i.e., orthogonal) cone-cylinder nets. Hereafter we use some terminology from differential geometry; see e.g. [26].

Proposition 16. *Regular smooth orthogonal cone-cylinder nets without umbilics are exactly principal curvature nets on cylinders, cones, and rotational surfaces without umbilics.*

Proof. Clearly, such principal curvature nets are smooth orthogonal cone-cylinder nets.

Conversely, consider any regular smooth orthogonal cone-cylinder net without umbilics. By Proposition 14, the tangents to the u-parameter lines at points of each v-parameter line are concurrent or parallel and the tangents to the v-parameter lines at points of each u-parameter line are parallel. By orthogonality, each v-parameter line lies on a sphere or a plane S_v orthogonal to the u-parameter lines (at the points of the v-parameter line), and each u-parameter line lies on a plane P_u orthogonal to the v-parameter lines. We get a strong restriction on the net in each of the possible cases:

Case 1: all the planes P_u are parallel. Each v-parameter line is orthogonal to one of the planes P_u at each point, hence it is a straight line orthogonal to them. We get a principal curvature net on a cylinder.

Case 2: all the planes P_u have a common line l. Each v-parameter line is orthogonal to one of the planes P_u at each point, hence it is a circle with the axis l. We get a principal curvature net on a rotational surface.

Case 3: some three planes P_u have a unique common point or intersect in three parallel lines. By construction, each sphere or plane S_v is orthogonal to each plane P_u. Therefore, if S_v is a sphere, then its center belongs to the intersection of all the planes P_u. If some three planes P_u pairwise intersect in three parallel lines, then the triple intersection is empty, and all S_v must be parallel planes. Interchanging u and v leads to Case 1 already considered. If some three planes P_u have a unique common point, then all S_v must be concentric spheres. Each u-parameter line is orthogonal to one of the spheres S_v at each point, hence it is a straight line passing through their common center. We get a principal curvature net on a cone. □

This can also be deduced from a theorem by Darboux [26, Theorem 16]. It would be interesting to obtain an analogous result in the discrete setup. Cf. [26, Theorem 38].

5. Conclusion, Flexible Nets, and Future Work

Motivated by the design of flexible Q-nets in Euclidean geometry, we first turned to the isotropic counterpart and, more precisely, to the metric dual in I^3. These dual nets are Q-nets which are deformable in the sense that they admit a one-parameter family of area preserving Combescure transformations. Using elementary algebraic and geometric methods, we could completely classify these nets. They fall into two classes. Class (i) is composed of two interleaved cone-cylinder nets. Class (ii) is characterized by the existence of a Christoffel dual with equal areas of corresponding faces. This implies, in general, a visually non-smooth behavior. As a result of that, the smooth analogs of (ii) are just translational nets and a special case of the smooth analogs of type (i), which are smooth cone-cylinder nets, also known as scale-translational surfaces.

While the Euclidean classification of flexible Q-nets has so far only been done for nets with 3×3 faces and led to a large number of classes [10], the isotropic classification is for arbitrary $m \times n$ nets and has only two classes.

5.1. Flexible Nets in I^3

Let us briefly and informally mention some basic facts on flexible conjugate nets in isotropic 3-space I^3 (both smooth and discrete). They are related to the deformable nets studied in this paper through metric duality. This duality can be realized by polarity with respect to the *isotropic unit sphere* $S_i^2 : 2z = x^2 + y^2$, which is a rotational paraboloid in Euclidean space with Cartesian coordinates (x, y, z). It maps a point with coordinates (u, v, w) to a plane and vice versa:

$$\delta\colon (u, v, w) \longleftrightarrow ux + vy - z - w = 0.$$

Parallel planes $ux + vy - z - w_i = 0,\ i = 1, 2$, correspond to points (u, v, w_i) with the same projection $(u, v, 0)$ onto the plane $z = 0$ (*top view*). Note that isotropic distances are measured in the top view. A smooth surface f seen as a set of contact elements (p, T) (points plus tangent planes) gets mapped to a surface $\delta(f)$ as a set of contact elements $(\delta(p), \delta(T))$ (tangent planes plus contact points). If K_i is the isotropic Gaussian curvature at a contact element of f, the isotropic Gaussian curvature at the image element is $1/K_i$ [38]. For a deformation of f, both are preserved by Remark 6. Putting all these facts together, we see that *a smooth deformable net f corresponds under metric duality δ to a flexible net $\delta(f)$*: The deformation keeps the top view (thus the intrinsic metric) and the isotropic Gaussian curvature invariant. This characterizes an isometric deformation in I^3 (see [20]). By definition, *a deformable*

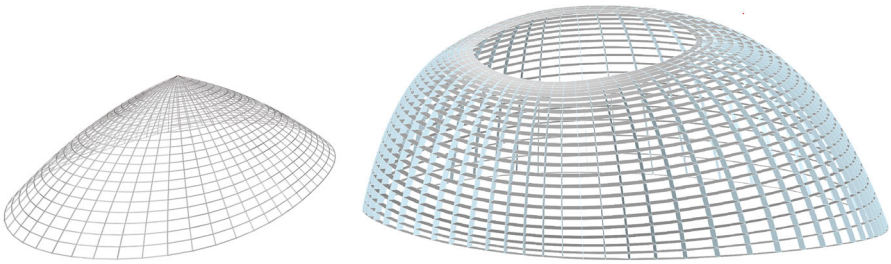

FIGURE 18. A cone-cylinder net (left) and its metric dual (right). The latter is a flexible surface in isotropic geometry having planar discrete parameter lines, one family lying in isotropic planes. Parts of those planes are shown in the figure to the right

Q-net f corresponds under metric duality δ to a flexible Q-net $\delta(f)$. If a Q-net f is deformable, so are all Q-nets that have the same top view as f. Via duality, we obtain the expected isotropic counterpart of a property of flexible Q-nets in Euclidean $\mathbb{R}^3$: *If a Q-net is flexible in I^3, so are all nets related to it by Combescure transformations.*

Let us briefly discuss the dual $\delta(f)$ of a discrete cone-cylinder net f. Any polarity relates lines through a fixed point to lines in a fixed plane. In particular, δ maps parallel lines to lines with the same top view. Thus, a cone-cylinder net corresponds to *a Q-net with planar parameter lines, where one family of parameter lines lie in isotropic planes (parallel to the z-axis)*. This family corresponds to the cylindrical strips. The parameter lines of the other family do, in general, not lie in isotropic planes. Only a translational net f corresponds to a Q-net where both families of parameter lines lie in isotropic planes. These are the isotropic counterparts to Voss nets (see also [20]). Note that the class of Q-nets whose parameter lines lie in planes is invariant under C-trafos and so is the property of parameter lines lying in isotropic planes.

Even without the isotropic flexibility, the nets $\delta(f)$ are of interest for applications, namely in architectural structures. The planarity of faces (panels) and of parameter lines (long range supporting beams) provides an advantage for construction (see [29,30]). If we consider the z-axis vertical, one family of these long range beams lies in vertical planes, which can be an advantage as well. An example is shown in Fig. 18.

5.2. Future Research

In a subsequent paper, we will discuss flexible nets in I^3 in detail. As a conclusion from the present study, we know already that the only nets with a visually smooth appearance can be those of class (i). However, flexible mechanisms often have a folding behavior, and therefore we also need to address class (ii). From a geometric perspective, it is interesting to study the reciprocal parallel

nets of flexible nets in I^3. Their Euclidean counterparts (Bianchi surfaces in the smooth setting) have been addressed by Schief et al. [33]. On the applications side, the main focus is on good ways to control the shapes of flexible Q-nets in I^3 and on numerical optimization algorithms for the transition to flexible Q-nets in Euclidean 3-space. Our initial numerical experiments show that this transition works for Voss nets, and thus we are optimistic that the more interesting general types can be handled as well. The isotropic flexible Q-nets are more general than just isotropic counterparts to the explicitly known Euclidean flexible $m \times n$ nets (Voss nets, T-nets and P-nets [12]). Possibly the simpler isotropic versions lead to so far unknown explicit constructions of certain types of Euclidean flexible Q-nets that do not require numerical optimization.

The idea of initializing a numerical optimization algorithm for the computation of a Euclidean structure by an isotropic counterpart goes beyond the context of flexibility and deserves to be investigated for other difficult problems. For instance, see [39,40].

Acknowledgements

The authors are grateful to Niklas Affolter, Mekhron Bobokhonov, Alexander Fairley, Ivan Izmestiev, Oleg Karpenkov, Naimdzhon Khondzhonov, Niels Lubbes, Dmitry Lyakhov, Christian Müller, Klara Mundilova, and Florian Rist for useful discussions.

Author contributions All authors contributed equally to this work.

Funding This research work has been supported by KAUST baseline funding.

Data Availibility Data sharing is not applicable to this article as no datasets were generated or analyzed during the current study.

Declarations

Conflict of interest The authors have no relevant financial or non-financial interests to disclose.

References

[1] Aikyn, A., Liu, Y., Lyakhov, D.A., Rist, F., Pottmann, H., Michels, D.L.: Flexible Kokotsakis meshes with skew faces: generalization of the orthodiagonal involutive type. Comput. Aided Des. **168**, 103669 (2024)

[2] Chen, Y., Peng, R., You, Z.: Origami of thick panels. Science **349**(6246), 396–400 (2015)

[3] Dang, X., Feng, F., Plucinsky, P., James, R.D., Duan, H., Wang, J.: Inverse design of deployable origami structures that approximate a general surface. Int. J. Solids Struct. **234**, 111224 (2022)

[4] Feng, F., Dang, X., James, R.D., Plucinsky, P.: The designs and deformations of rigidly and flat-foldable quadrilateral mesh origami. J. Mech. Phys. Solids **142**, 104018 (2020)

[5] Evans, T.A., Lang, R.J., Magleby, S.P., Howell, L.L.: Rigidly foldable origami gadgets and tessellations. R. Soc. Open Sci. **2**(9), 150067 (2015)

[6] Lewis, R.H., Coutsias, E.A.: Flexibility of Bricard's linkages and other structures via resultants and computer algebra. Math. Comput. Simul. **125**, 152–167 (2016)

[7] Nawratil, G.: On continuous flexible Kokotsakis belts of the isogonal type and V-hedra with skew faces. J. Geom. Graphics **26**(2), 237–251 (2022)

[8] Sharifmoghaddam, K., Nawratil, G., Rasoulzadeh, A., Tervooren, J.: Using flexible trapezoidal quad-surfaces for transformable design. In: Proceedings of IASS Annual Symposia, vol. 2020 (International Association for Shell and Spatial Structures (IASS), 2020), pp 1–13

[9] Tachi, T.: Generalization of rigid foldable quadrilateral mesh origami. J. Int. Ass. Shell Spat. Struct. **50**, 173–179 (2009)

[10] Izmestiev, I.: Classification of flexible Kokotsakis polyhedra with quadrangular base. Int. Math. Res. Not. **2017**(3), 715–808 (2017)

[11] Sauer, R.: Differenzengeometrie. Springer (1970)

[12] Nawratil, G.: From axial C-hedra to general P-nets. In: International Symposium on Advances in Robot Kinematics. pp. 340–347, Springer (2024)

[13] He, Z., Guest, S.D.: On rigid origami II: quadrilateral creased papers. Proc. R. Soc. A **476**(2237), 20200020 (2020)

[14] Müntz, C.: Zum Randwertproblem der partiellen Differentialgleichung der Minimalflächen. J. Reine Angew. Math. **139**, 52–79 (1911)

[15] Strubecker, K.: Differentialgeometrie des isotropen Raumes I: Theorie der Raumkurven. Sitzungsber. Akad. Wiss. Wien **150**, 1–53 (1941)

[16] Strubecker, K.: Differentialgeometrie des isotropen Raumes II: Die Flächen konstanter Relativkrümmung $K = rt - s^2$. Math. Zeitschrift **47**, 743–777 (1942)

[17] Strubecker, K.: Differentialgeometrie des isotropen Raumes III: Flächentheorie. Math. Zeitschrift **48**, 369–427 (1942)

[18] Strubecker, K.: Differentialgeometrie des isotropen Raumes IV: Theorie der flächentreuen Abbildungen der Ebene. Math. Zeitschrift **50**, 1–92 (1944)

[19] Sachs, H.: Isotrope Geometrie des Raumes. Vieweg (1990)

[20] Müller, C., Pottmann, H.: Isometric surfaces in isotropic space (2024)

[21] Bobenko, A., Suris, Yu.: Discrete differential geometry: Integrable Structure. No. 98 in Graduate Studies in Math. (American Math. Soc., 2008)

[22] Fubini, G.: Il parallelismo die Clifford negli spaci ellittici. Annali Reale scuola norm. sup. Pisa **9**, 1–74 (1904)

[23] Müller, H.R.: Sphärische Kinematik. VEB Deutscher Verlag d. Wiss. (1962)

[24] Pottmann, H., Wallner, J.: Computational Line Geometry. Springer (2001)

[25] Scheffers, G.: Flächentreue Abbildungen in der Ebene. Math. Zeitschrift **2**, 180–186 (1918)

[26] Kilian, M., Müller, C., Tervooren, J.: Smooth and discrete cone-nets. RM **78**(3), 110 (2023)

[27] Glympf, J., Shelden, D., Ceccato, C., Mussel, J., Schober, H.: A parametric strategy for free-form glass structures using quadrilateral planar facets. Autom. Constr. **13**, 187–202 (2004)

[28] Bobenko, A., Pottmann, H., Rörig, T.: Multi-nets: Classification of discrete and smooth surfaces with characteristic properties on arbitrary parameter rectangles. Discret. Comput. Geom. **63**, 624–655 (2020)

[29] Jiang, C., Wang, C., Tellier, X., Wallner, J., Pottmann, H.: Planar panels and planar supporting beams in architectural structures. ACM Trans. Graphics **42**(2), 1–17 (2022)

[30] Wang, C., Jiang, C., Wang, H., Tellier, X., Pottmann, H.: Architectural structures from quad meshes with planar parameter lines. Comput. Aided Design **156**, 103463 (2023)

[31] Morozov, E.A.: Symmetries of 3-polytopes with fixed edge lengths. Sib. Electron. Math. Rep. **17**, 1580–1587 (2020). https://doi.org/10.33048/semi.2020.17.110

[32] Karpenkov, O.N.: On the flexibility of Kokotsakis meshes. Geom. Dedicata. **147**(1), 15–28 (2010)

[33] Schief, W.K., Bobenko, A.I., Hoffmann, T.: On the integrability of infinitesimal and finite deformations of polyhedral surfaces. Discrete Differ. Geom. 67–93 (2008)

[34] Bobenko, A.I., Pottmann, H., Wallner, J.: A curvature theory for discrete surfaces based on mesh parallelity. Math. Ann. **348**, 1–24 (2010)

[35] Grünbaum, B., Shephard, G.C.: Ceva, Menelaus, and the area principle. Math. Mag. **68**(4), 254–268 (1995)

[36] Pirahmad, O., Skopenkov, M.: Area preserving Combescure transformations: Auxiliary computations. https://github.com/17199197/Area-preser-Comb-transf.git (2024)

[37] Izmestiev, I., Rasoulzadeh, A., Tervooren, J.: Isometric deformations of discrete and smooth T-surfaces. Comput. Geom. **122**, 102104 (2024)

[38] Strubecker, K.: Duale Minimalflächen des isotropen Raumes. Rad JAZU **382**, 91–107 (1978)

[39] Morozov, E.: Surfaces containing two isotropic circles through each point. Comput. Aided Geom. Design **90**, 102035 (2021). https://doi.org/10.1016/j.cagd.2021.102035

[40] Yorov, K., Skopenkov, M., Pottmann, H.: Surfaces of constant principal-curvatures ratio in isotropic geometry. Beitr. Algebra Geom. (2024). https://doi.org/10.1007/s13366-024-00768-5

Olimjoni Pirahmad, Helmut Pottmann and Mikhail Skopenkov
CEMSE
King Abdullah University of Science and Technology, KAUST
23955-6900 Thuwal
Saudi Arabia
e-mail: pirahmad.olimjoni@kaust.edu.sa;
helmut.pottmann@gmail.com;
mikhail.skopenkov@gmail.com

Helmut Pottmann
Institute of Discrete Mathematics and Geometry
TU Wien
Wiedner Hauptstr. 8-10
1040 Wien
Austria

Received: February 28, 2024.
Accepted: December 21, 2024.